Cell

Reshaping Antibody Diversity

Feng Wang,[1,8,9] Damian C. Ekiert,[2,8] Insha Ahmad,[3] Wenli Yu,[2] Yong Zhang,[1] Omar Bazirgan,[5] Ali Torkamani,[4] Terje Raudsepp,[6] Waithaka Mwangi,[7] Michael F. Criscitiello,[7] Ian A. Wilson,[2,*] Peter G. Schultz,[1] and Vaughn V. Smider[3,5,*]
[1]Department of Chemistry
[2]Department of Integrative Structural and Computational Biology
[3]Department of Cell and Molecular Biology
[4]Department of Molecular and Experimental Medicine
The Scripps Research Institute, La Jolla, CA 92037, USA
[5]Fabrus, Inc., La Jolla, CA 92037, USA
[6]Department of Veterinary Integrative Biosciences
[7]Department of Veterinary Pathobiology
College of Veterinary Medicine and Biomedical Sciences, Texas A&M University, College Station, TX 77843, USA
[8]These authors contributed equally to this work
[9]Present address: California Institute for Biomedical Research, La Jolla, CA 92037, USA
*Correspondence: wilson@scripps.edu (I.A.W.), vvsmider@scripps.edu (V.V.S.)
http://dx.doi.org/10.1016/j.cell.2013.04.049

SUMMARY

Some species mount a robust antibody response despite having limited genome-encoded combinatorial diversity potential. Cows are unusual in having exceptionally long CDR H3 loops and few V regions, but the mechanism for creating diversity is not understood. Deep sequencing reveals that ultralong CDR H3s contain a remarkable complexity of cysteines, suggesting that disulfide-bonded minidomains may arise during repertoire development. Indeed, crystal structures of two cow antibodies reveal that these CDR H3s form a very unusual architecture composed of a β strand "stalk" that supports a structurally diverse, disulfide-bonded "knob" domain. Diversity arises from somatic hypermutation of an ultralong DH with a severe codon bias toward mutation to cysteine. These unusual antibodies can be elicited to recognize defined antigens through the knob domain. Thus, the bovine immune system produces an antibody repertoire composed of ultralong CDR H3s that fold into a diversity of minidomains generated through combinations of somatically generated disulfides.

INTRODUCTION

Antibodies are quite diverse, but this heterogeneity is present within the constraints of the immunoglobulin fold. The most diverse portion of the antibody molecule is the complementarity determining region 3 of the heavy chain (CDR H3), which is derived from DNA rearrangement of variable (V), diversity (D), and joining (J) gene segments (Fugmann et al., 2000; Kato et al., 2012; Smider and Chu, 1997). Additional point mutations are acquired in the variable regions after antigen exposure through somatic hypermutation (SH) (Di Noia and Neuberger, 2007; Kocks and Rajewsky, 1988). Despite the genetic modifications of gene rearrangement and SH, the overall structure of the antibody is maintained within the immunoglobulin fold and the associated CDR loops of the heavy and light chains. Variations on this theme include V_{HH} antibodies from camelids and the IgNAR of sharks (Decanniere et al., 1999; Stanfield et al., 2004), which contain bivalent heavy-chain domains without light chains; however, both of these still utilize their heavy-chain CDR loops to bind antigen. The only known exception to this structural paradigm for antigen recognition is the variable lymphocyte receptor of jawless vertebrates, which use a leucine-rich repeat scaffold with variable loops to bind antigen (Alder et al., 2005; Pancer et al., 2004; Han et al., 2008). Interestingly, some vertebrates, such as *Bos taurus*, have a very limited diversity of V gene segments (Berens et al., 1997; Lopez et al., 1998; Saini et al., 2003; Sinclair et al., 1997; Zhao et al., 2006) yet maintain a perfectly robust adaptive immune response, suggesting unique diversification mechanisms at work to generate a functional antibody repertoire.

The CDR H3 is typically 8–16 amino acids in length in humans (Figure 1A) and, along with the other CDRs of the heavy and light chain, usually forms a flat or undulating binding surface for antigen recognition. In humans, some longer CDR H3 loops with unusual protruding structures have been described that contribute to important functions such as virus neutralization (Collis et al., 2003; Kwong and Wilson, 2009; Pejchal et al., 2010; Saphire et al., 2001; McLellan et al., 2011; Ekiert et al., 2012). Different species exhibit a diversity of CDR H3 length; however, bovine antibodies have the longest CDR H3 regions known, with an ultralong subset that ranges in length from 50 to 61 amino acids (Berens et al., 1997; Lopez et al., 1998; Saini et al., 1999, 2003; Zhao et al., 2006) (Figure 1A). These heavy chains pair with a restricted set of lambda light chains (Saini et al., 2003) and have multiple but an even number of cysteines, suggesting that they participate in disulfide bonds (Saini et al., 1999) (Figure 1B). The restricted V_H-V_L pairing, potential for multiple disulfide bonds, and the unusually long length suggests that these bovine CDR H3s might not be simple loops or β-hairpins

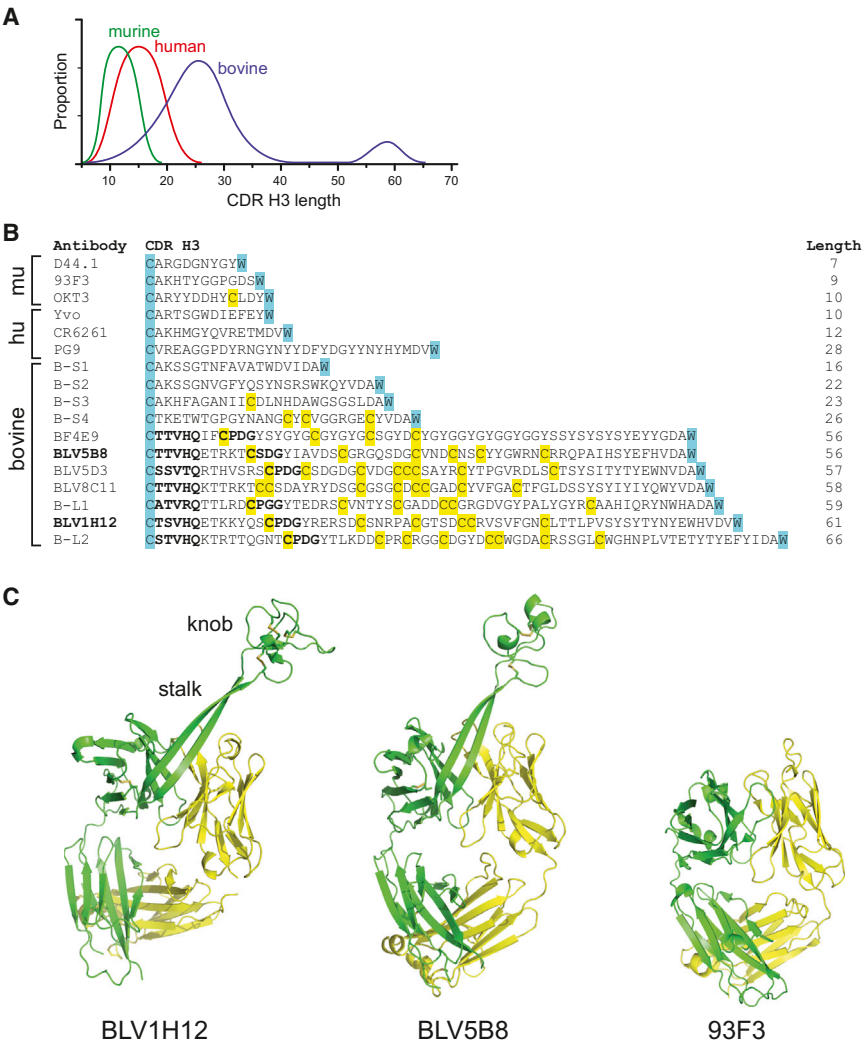

Figure 1. Identification of a Unique Structural Domain in Bovine Antibodies

(A) Comparison of CDR H3 length among murine, human, and bovine repertoires. An ultralong subset of more than 60 amino acids is uniquely found in bovine heavy chains (blue).

(B) Sequences of representative CDR H3s from murine (mu), human (hu), or bovine sequences from the literature along with six bovine sequences (B-S1 to B-S4 and B-L1 and B-L2) from our sequencing results. The conserved cysteine of framework 3 and tryptophan of framework 4 that define CDR H3 boundaries in all antibody variable regions are highlighted in cyan for reference, and cysteines are yellow. The lengths of the CDR H3s are indicated at the right. The murine antibodies include D44.1, an anti-HEL antibody, 93F3, an aldolase, and OKT3, a therapeutic antibody targeting human CD3. The OKT3 antibody is unusual in having a free cysteine in CDR H3. The human antibodies include Yvo, a cryoglobulin, CR6261, an anti-influenza A hemaglutinin, and PG9, an anti-HIV antibody that has one of the longest human CDR H3s. The bovine antibodies represent the ultralong sequences in the literature, and short sequences for comparison. BLV5B8 and BLV1H12 (indicated in bold) were used in our structure determinations. Relatively conserved TTVHQ and CPDG motifs are in bold.

(C) Crystal structures of BLV1H12 (left) and BLV5B8 (middle) Fabs compared to the 93F3 Fab with a "normal" CDR H3 (right). A superlong, two-β-stranded stalk protrudes from each bovine V_H immunoglobulin domain and terminates in an unusual three disulfide-linked knob domain.

See also Figure S1 and Table S1.

but that they have a unique and well-defined structural fold. Although they represent more than 10% of the bovine repertoire, the structure, function, and underlying genetic mechanisms resulting in ultralong CDR H3 formation and diversity generation have not been elucidated.

RESULTS

A Unique Antibody Structure in Cattle

To delineate the architecture of bovine antibodies containing ultralong CDR H3s, we determined crystal structures of two Fab fragments: BLV1H12 and BLV5B8 (Table S1 available online). Each of these antibodies was originally cloned from a fetal calf infected with bovine leukemia virus (which transforms B cells); however, the original antigens eliciting these antibodies are unknown (Saini et al., 1999, 2003). The CDR H3s of BLV5B8 and BLV1H12 are 56 and 61 amino acids, respectively (Figure 1B). The overall structure of the BLV1H12 variable region core is very similar to other antibodies except for the CDRs of the heavy and light chains (Figure 1C). The 61 residue CDR H3 forms an unprecedented structure in which a subdomain with an unusual architecture is formed from a "stalk," composed of two 12-residue, antiparallel β strands, and a 39 residue, disulfide-rich "knob" that sits atop the stalk far from the canonical antibody paratope (Figure 1C, left). The long antiparallel β ribbon serves as a bridge to link the "knob" domain with the main antibody scaffold and is rigidified using eight standard β sheet hydrogen bonds. The CDR H3 of a second antibody, BLV5B8, has little sequence homology to BLV1H12, but the unique "stalk" and "knob" structural features are maintained (Figure 1C, middle). The two bovine antibodies have dramatically different CDR H3 structures compared to a typical CDR H3 in mouse or human antibodies (Figure 1C, right).

Structural Diversity in Bovine CDR H3s

Both BLV1H12 and BLV5B8 have stalk and knob components that share certain features, including a "T(T/S)VHQ" motif at the base of the ascending strand, which is connected by a variable number of residues to a "CPDG" motif (CSDG in BLV5B8) that forms a β-turn at the base of each knob (Figure 1B). These motifs are generally conserved in ultralong CDR H3s of bovine antibodies (Figure 1B). Detailed examination, however, reveals that the stalk and knob conformations are otherwise distinct

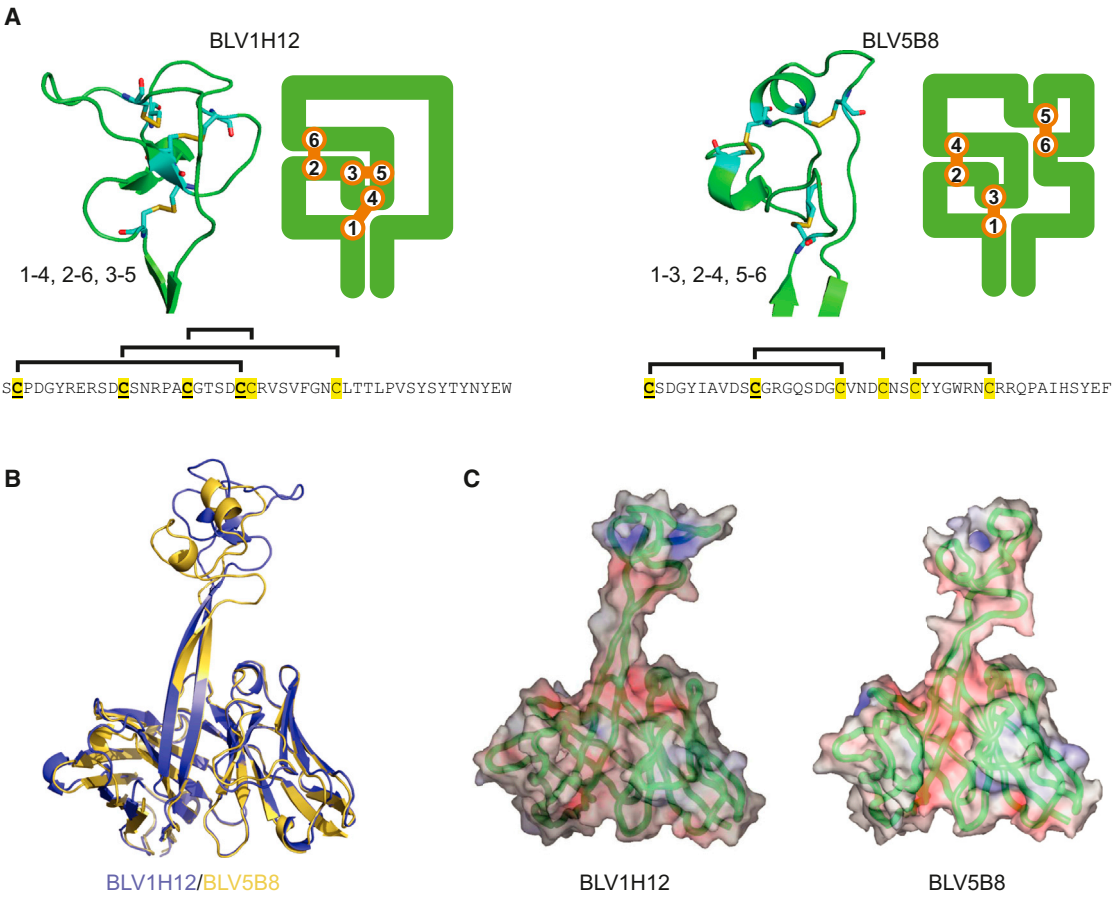

Figure 2. Structural Diversity in Ultralong Bovine Antibodies

(A) Comparison of the structure of the two knobs showing differences in disulfide patterns. Close up views of the knobs of BLV1H12 (left) and BLV5H8 (right) are shown, in addition to a two-dimensional representation of the knob and its disulfide pattern. Disulfides are in orange. The sequences of the knob regions are shown below, with cysteines in yellow and those conserved with the D_H2 germline gene segment underlined. The disulfide pattern is indicated above each sequence.

(B) Overlay of the variable regions of BLV1H12 (blue) and BLV5B8 (yellow) shows structural homology in the variable regions except the upper part of the stalk and knob, which are significantly divergent.

(C) Surface and charge density representation of BLV1H12 (left) and BLV5B8 (right) showing different shapes and charge in the knob region. The Cα backbone is in green, surface positive charge is in blue, and negative charge is in red.

due to different disulfide bond patterns and low amino acid sequence identity. The 39-residue knob domain of BLV1H12 is composed of two short, antiparallel β strands surrounded by three loops and folded such that three disulfide bonds adopt a 1-4, 2-6, 3-5 pattern (Figure 2A, left), which is rarely seen in protein structures. In contrast, the 37 residue knob of BLV5B8 is composed of three loops and two short α helices and folded such that three disulfide bonds form a 1-3, 2-4, 5-6 pattern (Figure 2A, right). The stalk can be of variable length (Figure 1B); BLV5B8 is two residues shorter than BLV1H12, which reorients the stalk at its distal end and alters the relative position and orientation of the knob domain (Figure 2B). The surface potentials of the two knobs are different, with BLV1H12 generally more positively charged due to frequent occurrence of arginine (Figure 2C). A search of the Dali protein structure database did not reveal any structurally similar domains to either knob. The ascending β strand contains mainly hydrophilic side chains, whereas the descending strand of the stalk is "YTYNY" in BLV1H12 and "HSYEF" in BLV5B8, where the alternating aromatics form a ladder through stacking interactions. Other ultralong sequences (Figure 1B and below) share this motif of alternating aromatics (often YxYxY), suggesting that this structural feature is important for integrity of the stalk. This unique amino acid pattern may contribute to the stability of this long solvent-exposed, two-stranded β ribbon (Richardson and Richardson, 2002). With the significant CDR H3 amino acid sequence differences and disulfide patterns, the fold, surface contour, and electrostatic properties of the BLV1H12 and BLV5B8 knob domains are distinct, yet both contain the key structural features of "stalk" and "knob" (Figures 1B and 2).

Genetic Basis Underlying Ultralong CDR H3 Structure

The unique disulfide-bonded structures of BLV1H12 and BLV5B8 pose the question as to how such sequences arise

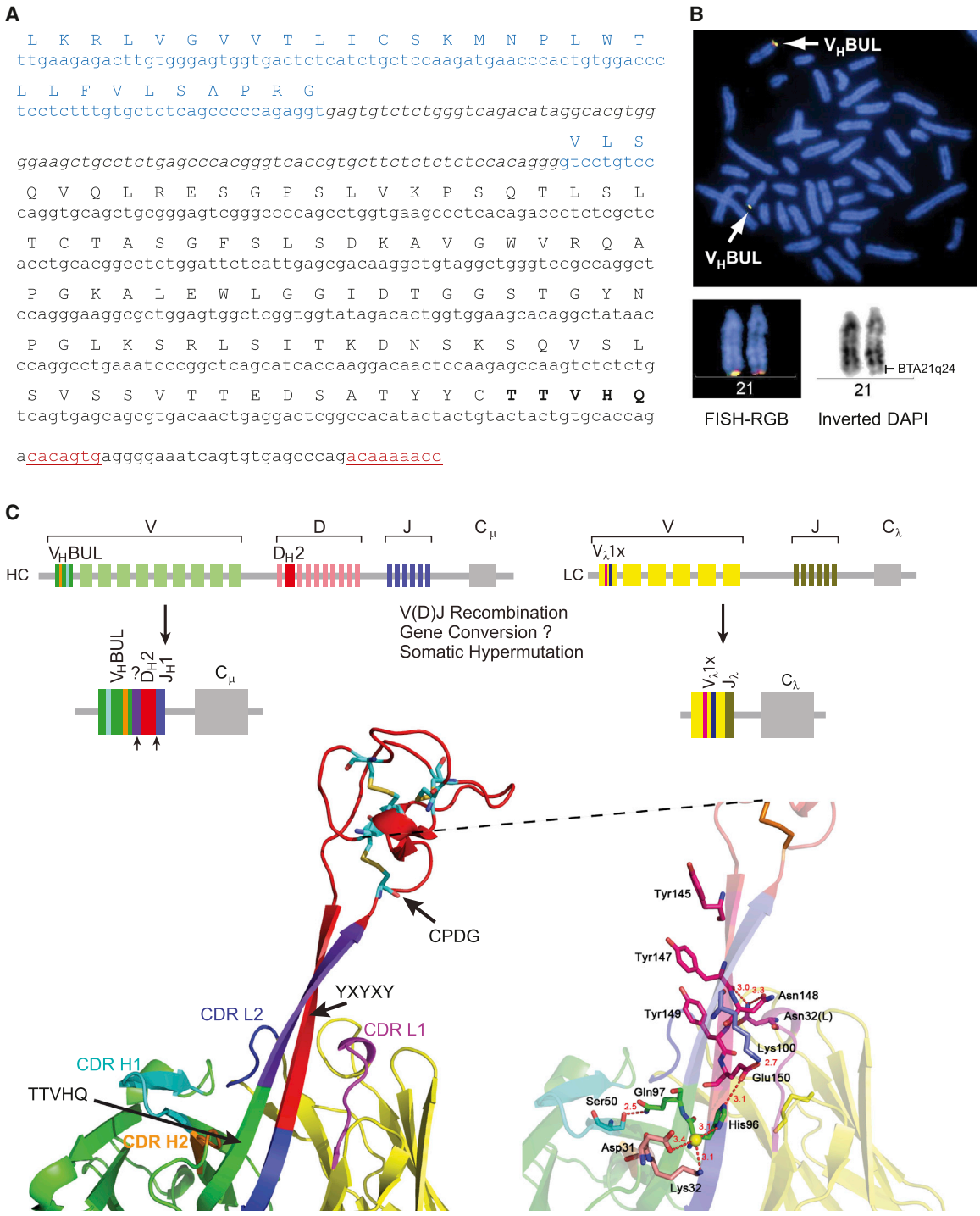

Figure 3. Genetic Basis for Ultralong Antibody Formation

(A) Identification of V_HBUL, a germline variable region used in ultralong antibodies. The leader sequence is in blue, the coding sequence is indicated with the amino acid translation above, the intron is in italics, and the unique TTVHQ extension, which forms a portion of the ascending strand of the stalk, is in bold. The recombination signal sequence heptamer and nonamer are underlined in red.

(B) The V_HBUL region is found on chromosome 21. Partial cattle metaphase spread (top) and enlarged chromosome 21 (bottom) showing the location of V_HBUL region in BTA21q24 by two-color FISH with BAC clones 318H2 (green) and 14-74H6 (red). International nomenclature for BTA21 is depicted at the bottom.

(C) Schematic of the bovine immunoglobulin loci depicting V_HBUL, D_H2, and $V_\lambda1x$, which are preferentially used in ultralong antibodies. The process of V(D)J recombination assembles the gene segments to form functional ultralong heavy- and light-chain genes. (bottom left). The V-D-J regions mapped onto the BLV1H12 Fab structure. Colors of the gene segments correlate with the colors of the structure. V_HBUL is unique in encoding CDR H1 and CDR H2 residues that

(legend continued on next page)

in vivo. Antibodies utilize V(D)J recombination and SH to produce diversity in the antibody repertoire. The V_H encodes the majority of the V region, D_H encodes a significant portion of CDR H3, and J_H encodes the terminal β strand. Although CDR H3s can vary in length, they are constrained by the germline-encoded lengths of the D_H regions and N or P nucleotide insertions, which usually only account for addition of a few amino acids. Additionally, cysteine residues in CDRs are not common, but when present, they are typically conserved between germline and affinity matured sequences (Almagro et al., 2012; Thomson et al., 2008).

Upon sequencing several bovine V regions from spleen and lymph node, we found that all sequences with ultralong CDR H3s (>50 amino acids) contained a relatively conserved "T(T/S)VHQ" motif that initiates the ascending strand of BLV1H12 and BLV5B8. This sequence is very unusual, as most human and mouse germline V regions encode AK or AR amino acids in this region, which immediately follows the second conserved cysteine in the V_H. A search of the bovine genome revealed a single unique germline V_H region, which we have termed V_HBUL (V_H *b*ovine *u*ltra*l*ong, Figure 3A), that is present at the immunoglobulin locus on chromosome 21 by FISH analysis and not at a previously proposed duplicated immunoglobulin locus on chromosome 11 (Hosseini et al., 2004) (Figure 3B). V_HBUL contains a functional promoter, leader, intron, and recombination signal sequence and uniquely encodes the terminal "TTVHQ" motif (Figure 3C, left), as well as CDR H1 and H2 motifs that directly interact with the stalk (Figure 3C).

In traditional antibodies, CDRs of the heavy and light chains are normally used for antigen binding. In BLV1H12 and BLV5B8, the CDR H3 stalk is surrounded by the five other CDRs. The base of the stalk interacts with CDRs H1, H2, L1, and L3 (Figure 3C, left). The BLV1H12 "TSVHQ" motif (TTVHQ in the V_HBUL germline) at the base of the ascending strand interacts with a "DKAVG" motif in CDR H1 that is also highly conserved in bovine antibodies with ultralong CDR H3s but is divergent from CDR H1 of bovine antibodies with shorter CDR H3s (Figure 1B). The alignment of the crystal structures of BLV1H12 and a typical antibody indicates that this CDR H1 motif is shifted toward the base of the ascending β strand of the stalk (Figure 3C, bottom). In BLV1H12, Asp31, Lys 32 (CDR H1), and His96 (CDR H3, in TSVHQ in the ascending β strand) form a hydrogen-bonding network via a water molecule (W286). Ala33 forms a pair of typical β-strand-like hydrogen bonds with His96. The conserved Gln97 (in TSVHQ) forms a close hydrogen-bond interaction (2.5 Å) with Ser50 in CDR H2. The descending β strand also forms extensive interactions, but with CDRs L1 and L3, which are derived from a lambda light chain, V_λx1. CDR L3 is rotated ~90° to accommodate the descending β strand compared to the search model. Asn32 (CDR L1) hydrogen bonds with the side chain and backbone oxygen of Asn148 and Tyr147, respectively, in the CDR H3 descending strand (Figure 3C, bottom right). These features are not found in the V_H regions of conventional antibodies but are highly conserved between BLV1H12, BLV5B8, and other ultralong sequences (see below) and are encoded in the bovine germline. We speculate that the V_HBUL—and the invariant light chain V_λ1x that pairs with ultralong heavy chains—evolved specifically to provide a structural framework to support the stalk and knob, whereas CDR H1 and H2 are not used to bind antigen but provide structural support for the ultralong CDR H3 stalk. Thus, the germline basis for encoding the base of the stalk structure appears to reside in the V_HBUL component of the ultralong CDR H3, with support from CDRs H1 and H2, as well as the CDRs of an invariant lambda light chain V_λx1.

The remaining portion of CDR H3 is composed of the knob, part of the ascending strand, and the descending strand of the stalk. CDR H3s are typically encoded by the D_H region. Cattle have ten D_H regions identified to date (Elsik et al., 2009; Koti et al., 2008, 2010), but only D_H2 is long enough to be the genetic basis behind ultralong CDR H3s. Although a draft of the *Bos taurus* genome is available (Elsik et al., 2009), the assembly of the immunoglobulin heavy-chain locus is incomplete, leaving open the possibility of undiscovered ultralong D regions. An initial alignment between D_H2, the available literature sequences, and our initial sequences indicated some limited conservation of the cysteines, but little overall sequence homology within CDR H3s (Figure S1). Nevertheless, the first cysteine in D_H2, which is part of the CPDG motif (Figure S1), is highly conserved in ultralong CDR H3s. Additionally, the YxYxY motif forming the descending strand is also encoded by the 3′ portion of D_H2 (Figure 3C). Thus, it appears that D_H2, (or other similar unidentified D_H regions) encodes the "knob" domain and the descending strand of the stalk (Figure 3C, red).

Bovine Ultralong CDR H3s Are Enormously Diverse

Despite similar overall "stalk and knob" architectures, BLV1H12 and BLV5B8 have different patterns of disulfide-bonded cysteines that arise from different cysteine sequence positions. The available ultralong CDR H3 sequences are highly diverse but with limited conservation to the germline D_H2, suggesting that they are either derived from different germline D_H regions (with cysteines encoded at different positions) or arose through SH or gene conversion from a single D_H. In humans, SH is temporally regulated and acts after the naive B cell encounters antigen, adding mutations that, through selection, increase the affinity of the antibody. In contrast, ruminants have very limited V_H germline diversity, and SH appears to act in the primary repertoire as a mechanism to generate further diversity prior to antigen exposure (Lopez et al., 1998; Zhao et al., 2006). If the cysteines in ultralong CDR H3s are encoded in the germline genome, then the number of different knob minifolds would be limited by the number of ultralong D_H regions in the genome. However, if cysteines arise de novo from one or a few D regions through SH or gene conversion, then the knob structural features could form

interact with the stalk (cyan and orange), as well as a TTVHQ motif that initiates the ascending β strand. Similarly, the V_λ1x light chain encodes CDR L1 and CDR L2 residues that interact with the stalk (magenta and blue). Arrows indicate areas of potential junctional diversity. Relatively long V-D insertions are indicated in purple. It is unclear whether this sequence results from N additions, gene conversion, or another mechanism. (bottom right). A detailed depiction of the interactions of CDR H1, H2, L1, and L2 with the stalk of BLV1H12, as well as the location of the YxYxY motif of the descending strand.
See also Table S4.

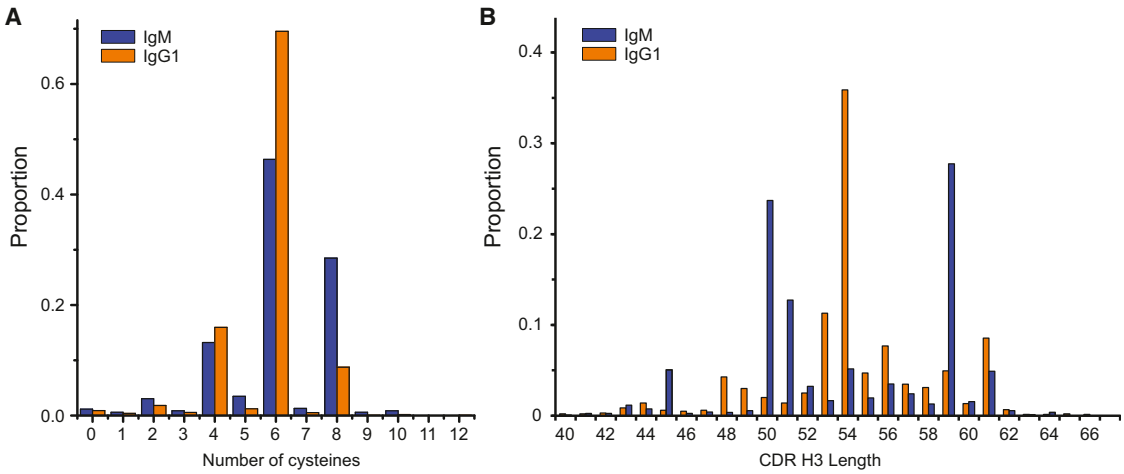

C

	V_H	N(?)	D_H	J_H	(L)
V_H Germ	CTTVHQ				
D_H2 Germ			SCPDGYSYGYGCGYGYGCSGYDCYGYGGYGGYGGYGYSSYSYSYTYEY		
J_H1 Germ				YVDAW	
BLV1H12	CTSVHQ	ETKKYQ	SCPDGYRERSDCSNRPACGTSDCCRVSVFGNCLTTLPVSYSYTYNYEW	HVDVW	61
BLV5B8	CTTVHQ	ETRKT	CSDGYIAVDSCGRGQSDGCVNDCNSCYYGWRNCRRQPAIHSYEF	HVDAW	56
(12 cys)	CSPVHQ	EIRK	CCPAGCQCGRSCGACCGCAGDEFCGINVYGYVTCGGYRTCSCIDTYDF	YVDAW	59
(10)	CTTVHQ	KTKK	LCPNGRTCGCGCDCGSGCCTSYCDSFGCWGGRDTFGSSCTSATYTYEW	GVDAW	59
(10)	CATVHQ	HTNKK	RCPDGYEFSAGCCCGEGCSGSDCCCNSRLRCSWYEIYCSVSPSDTYEF	HVDAW	60
(8)	CSTVHQ	KTRTTQGN	TCPDGYTLKDDCPRCRGGCDGYDCCWGDACRSSGLCWGHNPLVTETYTYEF	YIDAW	66
(8)	CTTVHQ	ETHKR	CPDGYTYGYYCGYACTCSGDECYRYDYCAAYGSLGCCTNDHTYTYEF	HVDSW	59
(6)	CTAVYQ	QTRK	SCPDGYRSGNDCSSACSCSNYECYRYGSYGSNGKCGYDAHAYTYTYEI	HIDAW	59
(6)	CGAVHQ	KTAR	SCPNIYSTYYGGRSGSVGCSAYDCENCCTYDGMGRYSVSTCSGSVIYEF	YVDTW	60
(6)	CATKKQ	I	CCPDDSSLEVACSHGAGCSGCVGYTGGTWGTLSDYFHGKYTCTYTYEH	NVDAW	56
(5)	CTIVHQ	QTTK	RCPDDDNYPYWCSVANGGGSDACYGCSGRSSDTFWRCSTVRYRYTYEW	HVDAW	59
(6)	CATVHQ	LTRA	HCPDDYSYLYTSRWDCASCDDGCYAARDWRGCFDCESSKTSVSYIYEH	HVNAW	59
(8)	CATVHQ	RTEK	SCCSAGHIDGVQCCCSGVACDGAGCVRGCSYGTDGWYGWCNRYSYTITYEF	YVTAW	61
(4)	CTTVHQ	RTKR	SCPDDYTYTYTCVSESDHQAERGCYGPGGYGWCDWTGSTTVSREGERNNYEF	HIDAW	63
(6)	CTTVHQ	ITHK	ECPDGYSDGCTCTRSWYYSGWNCYPGEVCWSRGGCGISGVTYSDTYEF	YIDAW	59
(8)	CGTVHQ	HTTTKN	TCPDGYTFRAGCCCSSGCISCDSSICDNTSPSWFCSRTSPTYTYTYEF	YITAW	61
(6)	CATVHQ	KTLEK	TCPDGYAYGDTDNGHCSAYDCWRMGTYCTEDMYGCSCYSGTTTYEW	YVEAW	58
(6)	CATVHQ	EVQKK	TCPDGYAHLGFCNDDDGRLGSACCSGGAFGSDGDTDCHCYSDSYNYEN	HVDEW	60
(6)	CSTVHQ	KTQR	SCPDGYRTGYGCDDGSCCSGSNCYSYLSRINRGTCRTKITTYEH	HIDAW	55
(7)	CTTVHQ	ETKTRS	TCPDGYGCTVGCYYGTYSCSGSDCTCSRIRRVYGATGGLSICTSTHTYEW	HVDTW	63
(4)	CTTVHQ	RTTTER	SCPEGYNWRYGCDGWVRGCSDACWTGDTDGARGEYGGDGSVRTSYEW	YADAW	60
(6)	CTTVHQ	KTQR	TCPDGWTDIWDCCRKSTCSGSDCPTNDDCRLIFPYAWSTTYLYTYEH	HVDTW	58

Figure 4. Deep Sequence Diversity of Bovine Ultralong V_H CDR H3s

(A) Distribution of the number of cysteines in bovine ultralong CDR H3s of IgM (blue) and IgG (orange).

(B) Length distribution of ultralong CDR H3s. Note that clonal sequences selected during an immune response can bias the proportion at any given length.

(C) Representative sequences of ultralong bovine V_H CDR H3s. The terminal portion of the V_HBUL region is shown, along with junctional diversity at the V-D joint, D_H2, and J_H (top). The sequences of BLVH12 and BLV5B8 are shown for comparison, followed by 20 ultralong CDR H3 sequences from IgG1 and IgM (bottom). Cysteines are in yellow, with those conserved with D_H2 underlined. The conserved cysteine and tryptophan that define the CDR H3 boundaries in all antibody variable regions are highlighted in cyan for reference. Note that the diversity of many of the cysteines is not conserved between the individual sequences or with D_H2. The CPDG motif is underlined in red, and the region of the descending strand encoding a possible YxYxY motif is underlined in blue.

See also Figure S1 and Tables S2, S3, and S5 for more sequence information.

dynamically during B cell development. These two mechanisms could potentially be distinguished by determining the sequence and cysteine diversity of the bovine ultralong CDR H3 repertoire.

To determine the diversity and content of ultralong bovine CDR H3s, we performed deep sequencing of bovine IgM and IgG variable region genes from two different cows and analyzed more than 10,000 ultralong CDR H3s (Figure 4, Supplemental Information, and Tables S2 and S3). Sequence analysis showed that an even number of cysteines was strongly preferred, suggesting that disulfides were formed in the knob region for nearly all ultralong CDR H3s (Figure 4A). Most sequences had 4, 6, or 8 cysteines, but 33 sequences had 10, and 2 sequences had 12 cysteines (Figure S1). The ultralong CDR H3s ranged in length from 40 to 67 residues (Figures 4B and S1), with the latter being the longest CDR H3 described to date (Figures 4C and S1). Interestingly, the CDR H3 length distribution is distinct between IgM

and IgG (Figure 4B). These lengths could be biased due to differential selection of clonally related sequences during an immune response or, alternatively, to other selection pressures such as stability or expression (Wang et al., 2013), which may be impacted by CDR H3 length. Several groups of clearly clonally related sequences were found that likely arose during ongoing SH. Among nonclonally related sequences, BLAST alignment did not reveal significant sequence conservation throughout the CDRs or positional conservation of the cysteines. However, when we fixed the first cysteine in each CDR H3 by aligning it with the germline D_H2, as in Figure S1, a pattern of conservation for several cysteines emerged that aligned with D_H2 (Figure 4C). However, many additional cysteines were not in positions encoded by germline D_H2 and did not appear conserved among the sequences (Figures 4C and S1). In one sequencing run, 655 out of 5,633 sequences had cysteines in different positions (Table S3), suggesting a significant potential for structural diversity based only on differing disulfide patterns. The sequences that did have a common cysteine pattern were often clearly clonally related, presumably the result of SH and selection in an immune response.

Cysteine Mutations Form Diversity in CDR H3

We reasoned that deep sequence analysis would reveal "clusters" of similar sequences if more than one D_H region was used to encode the ultralong CDR H3s. However, the sequences of the D_H formed only one cluster, without evidence for more than one significantly dissimilar D region (Figure S2), and the consensus sequences of the CDR H3s were highly homologous to D_H2, except for a portion at the very N terminus (Figure 5A). The overall consensus did not encode cysteines in positions divergent from D_H2. This result suggested that D_H2, or highly related homologs, are the germline precursors of the ultralong repertoire. Indeed, the nucleotide identity of the ultralong sequences to the germline D_H2 ranged from 35% to 75% (Supplemental Information and Figure S2). The D_H2 region encodes 48 amino acids with four cysteines and a repeating GYG motif (Figure 4C) that leads to a notable sequence bias with 17 tyrosines (35.4%), 14 glycines (31.3%), and 7 serines (14.6%). The limited homology among the deep sequences but with conservation of some cysteines (Figure 4C), along with the clustering of nearly 10,000 sequences to a consensus that was highly similar to the germline D_H2, suggested that extensive mutation from D_H2 could generate the remarkable diversity seen in the bovine repertoire. In this regard, the diversity of cysteines found in bovine ultralong CDR H3s is inconsistent with the known number of D_H regions in cattle or any mammalian species, further suggesting that they were somatically generated. Furthermore, the codon usages of the D_H2 germline residues are severely biased such that a single nucleotide mutation can produce a cysteine codon (Figure 5B). Indeed, an astonishing 39 of the 48 D_H2 residues (81%) can be mutated to cysteine with only one nucleotide change. The DNA sequence of D_H2 has numerous RGYW hotspots, which are known to be recognition motifs for the activation-induced (cytidine) deaminase (AID) that produces somatic mutations (Figure 5B). Thus, the DNA sequence of the germline D_H2 is primed for mutation to cysteine through SH.

To determine whether the cysteine diversity could be somatically generated, we analyzed clonally related sequences at various stages of somatic hypermutation (Figures 5C and S3). Indeed, we found Arg/Cys, Tyr/Cys, and Cys/Val mutations, directly demonstrating that cysteine patterns can be produced somatically. Because BLV1H12 and BLV5B8 have different disulfide patterns and because an even number of cysteines is strongly favored in our sequences (Figure 4A), the vast diversity of cysteine positions (Table S5) suggests that diverse combinations of disulfide bonds can be formed de novo using residues in D_H2, which are primed to mutate to cysteine through SH. Such mutations could occur through base pair changes (Figure 5C) or gene conversion events thought to occur in cattle (Parng et al., 1996), both of which are AID mediated. Irrespective of the mechanism, nucleotide changes resulting in addition or removal of cysteine codons can occur somatically and alter the pattern of cysteines in ultralong CDR H3s.

Antigen Binding of Ultralong CDR H3 Antibodies

The enormous diversity found in the ultralong repertoire suggested that these ultralong CDR H3 antibodies are a component of the adaptive immune response. To confirm that bovine antibodies utilize their ultralong CDR H3s to bind antigen, we immunized cattle with heat-killed bovine viral diarrhea virus (BVDV), a major bovine pathogen of worldwide agricultural economic importance (Figure 6). We collected lymphocyte messenger RNA (mRNA), amplified the variable regions, and paired the heavy-chain genes with the invariant lambda light chain to produce 132 recombinant bovine-human chimeric IgG (bovine V_H with human F_c) in microtiter wells (Mao et al., 2010). These IgGs were screened by ELISA for binding to BVDV, and several candidate binders were identified (Figure 6A). The H12 clone has a 63-residue CDR H3 with six cysteines (Figure 6B) and could strongly bind virus in a dose-dependent fashion (Figure 6A, right). We then overexpressed BVDV coat N^{pro}, structural (E2), and nonstructural (NS2-3) proteins on the surface of HEK293A cells and tested binding of B8 and H12 by immunocytometric analysis. H12 strongly binds HEK293A cells transfected with the NS2-3 nonstructural proteins of BVDV, which are required for production of infectious viral particles (Agapov et al., 2004) (Figure 6C), but binds extremely weakly to untransfected cells. As multiple clones derived from BVDV vaccinated cattle had ultralong CDR H3s with the same V_HBUL framework (and an identical light chain), the stalk and knob features in the ultralong CDR H3 antibodies appeared to mediate antigen binding.

To further understand the role of the stalk and knob in the binding mechanism of H12, we deleted the knob domain and replaced it with short SGS or SGGS linkers (Figure 6D). Removal of the knob domain completely abolished binding to BVDV (Figure 6D, left), suggesting that the majority of the antigen-binding activity resided in the knob. Next, we replaced approximately each third of the knob domain residues (109–148) with the irrelevant sequence ETYYGSGL and analyzed binding of the resulting mutant antibodies. Replacement of residues 109–117 had a minor impact on binding, whereas replacement of residues 119–129 reduced binding by more than 60%, and replacement of the distal residues 131–148 resulted in a complete loss in BVDV binding (Figure 6D, left). Although these wholesale swaps of

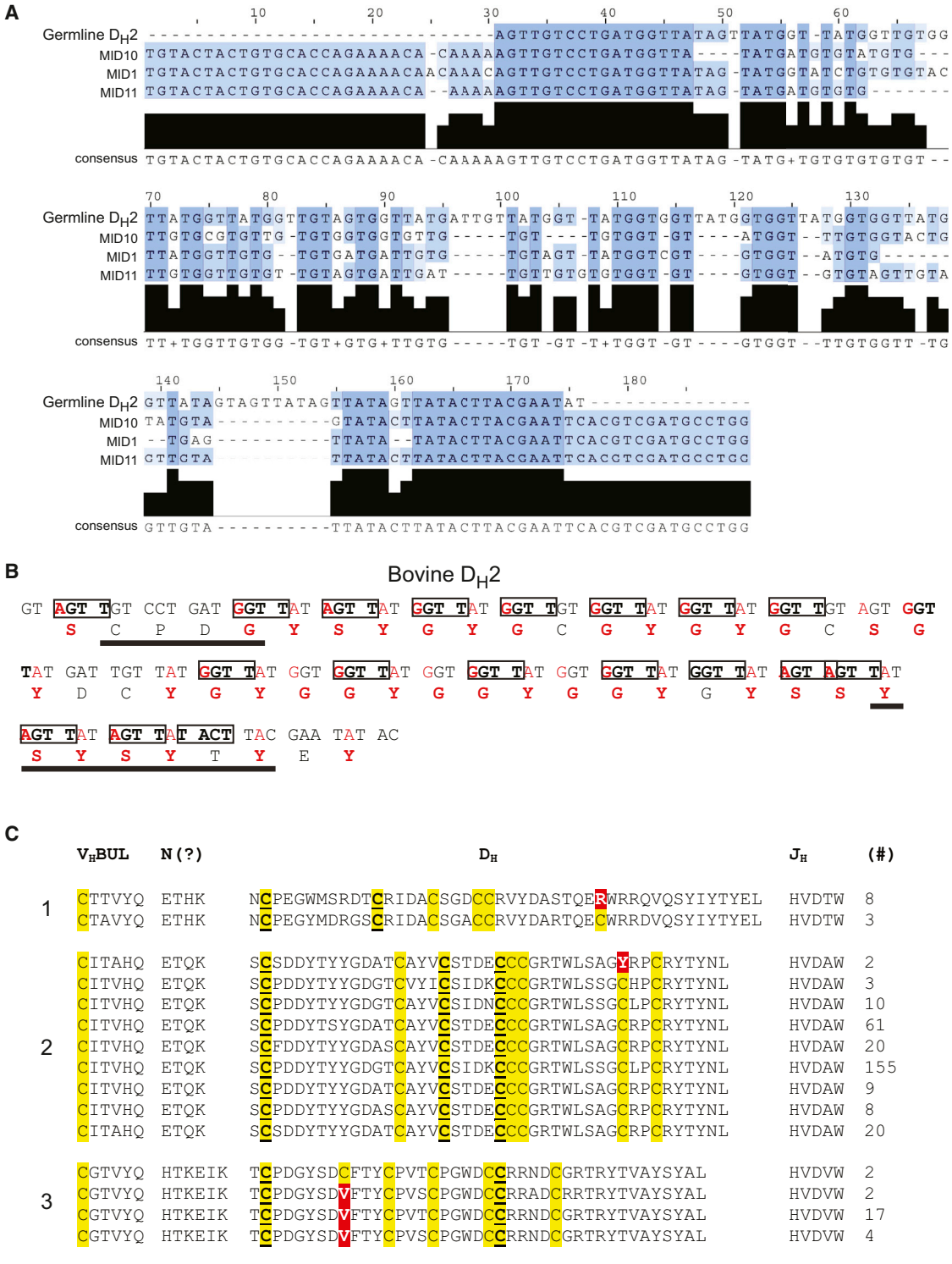

Figure 5. Cysteine Mutations Contribute to Ultralong CDR H3 Diversity

(A) The consensus of ultralong CDR H3 deep sequences aligns with D_H2. A consensus sequence for three deep sequencing runs (from two cows) were determined and were aligned with one another and with D_H2. The consensus aligns well except for some areas of insertions/deletions. Thus, either a single D_H gene, or highly related genes, produce the diversity of sequences in ultralong CDR H3 antibodies.

(B) D_H2 region analysis showing residues that can readily mutate to cysteine, including SH hot spots. The nucleotide sequence is above, and the translated amino acid sequence is below. RGYW hot spots, which are recognized by AID for SH and/or gene conversion, are boxed. Red nucleotides indicate positions that can be altered in a single mutation to a cysteine-encoding codon. Red amino acids are the corresponding residues that can be mutated to cysteine in a single step.

(legend continued on next page)

amino acid sequences could result in significant disruptions in folding of the knob, the results suggested that the N-terminal third of the knob is less important to BVDV binding than the C-terminal third. To further define the binding paratope, we generated alanine scan mutants of every residue in the knob domain except the three naturally occurring alanine residues (A110, A117, and A133), which were instead mutated to tyrosine. ELISA analysis of the mutants revealed a substantial decrease in BVDV binding for several residues between 134 and 145 (Figures 6D and S4), which is consistent with the complete loss of binding activity in the Δ131–148 replacement mutant. Indeed, within this stretch, only the relatively conservative G138A mutation retained binding activity. Other point mutations that inhibited binding by more than 80% included F112A, V116A, and R127A. Mutations like G111A and R113A in the N-terminal portion of the knob or V137A and Y141A near the C-terminal portion decreased binding by more than 60%. Several mutations had intermediary effects on binding, and others had no effect on binding (Figure 6D, right). The heatmap in Figure 6D clearly shows a significant impact of mutation of residues between 134 and 145, with other residues outside this region also playing a role in the binding or structural integrity of the knob domain, which may secondarily affect binding. Thus, in the case of H12, the C-terminal portion of the knob domain appears to mediate significant interaction with the BVDV antigen.

Although multiple ultralong CDR H3 sequences have been reported in the literature, the H12 antibody is the first antibody with an ultralong CDR H3 that binds a defined antigen, and we show here that this binding is clearly mediated through the knob domain, with little binding contributed by the stalk or the other five CDRs. Thus the bovine immune system creates a unique repertoire of mega CDR H3s—which fold into unusual stalk and knob structures that display a unique function in antigen recognition—through cysteine diversification.

DISCUSSION

A key component to the clonal selection theory of immune recognition is the generation of a diverse repertoire of antigen receptors. To create this diversity, some species have evolved multiple V, D, and J gene segments, which maximize combinatorial diversity. Other species, like chicken and rabbit, use a single V(D)J event followed by gene conversion to diversify the repertoire. Cows appear to be unique among higher vertebrates in evolving a new domain for antigen recognition and an unusual mechanism to create diversity in this architecture. Through a single V(D)J event, cows employ cysteine diversification to "reshape" the knob domain in ultralong CDR H3s, creating diverse structures for antigen binding.

Although BLV1H12 and BLV5B8 both contain a stalk with a distal disulfide-bonded knob domain, the ultralong CDR H3s were highly divergent in (1) sequence content, (2) disulfide bond pattern, and (3) stalk length. These diversity characteristics were also generally recapitulated in the bovine antibody repertoire sequences (Figures 4C and S1). The first cysteine in CDR H3 forms a disulfide bond at the base of the knob in both BLV1H12 and BLV5B8 and also is highly conserved in a "CPDG" motif in the ultralong deep sequence data. Thus, we could align all ultralong CDR H3s at this fixed cysteine. This alignment enabled visualization of residues most likely encoded by the V_HBUL, D_H, J_H, and putative N insertions. Notably, the length between the end of the V_HBUL and CPDG is variable due to differences in junctional diversity formed through V-D recombination. This region encodes a portion of the β strand ascending from the V_HBUL. Similarly, this change in length is matched through the D-J recombination event, which encodes the descending β strand of the stalk (Figure 3C). Of note, the YxYxY motif of the descending β strand is germline encoded in the D_H2 region, whereas a portion of the ascending strand does not appear to be encoded in the V_HBUL or D_H2 and could be the result of random N insertions, a proposed "oligonucleotide capture" mechanism (Koti et al., 2010), or gene conversion (Parng et al., 1996). Deep sequencing revealed some limited homology within the ascending strand among different antibodies; however, evidence for an alternative D region or D-D fusions has not been found. Although the combinatorial potential is severely limited, the natural diversity mechanism of V(D)J recombination can alter the length and orientation of the stalk, allowing the knob to protrude from the antibody at variable distances and geometries.

The bovine ultralong CDR H3 repertoire represents another paradigm for the generation of structural diversity by forming a unique architecture distinct from the immunoglobulin domain. Through X-ray crystallography and deep sequencing analysis, we demonstrate that the bovine antibody system utilizes V(D)J recombination and mutational mechanisms to produce CDR H3s with unique "minifolds" composed of a stalk and a knob, both of which can accommodate significant structural variation, including diverse disulfide-bond patterns and loop structures in the knob, as well as differences in length, orientation, and content of the stalk. The codons in the germline D region encoding ultralong bovine CDR H3s are severely biased toward mutation to cysteine, which may allow new disulfide bonds to be formed or broken in the knob. As both gene conversion and SH utilize AID to create diversity, we suspect that AID produces the remarkable diversity in bovine ultralong CDR H3s through one or both of these mechanisms. With mutation to and from cysteine, the disulfide pattern of germline antibodies, which encodes four cysteines in D_H2, is distinct from their mature counterparts. Thus, disulfide exchange may occur over time during development of the repertoire (Figure 7A and Table S6). This mechanism suggests ways for rapid minifold evolution in general; a primordial gene with a preferential mutational potential to cysteine could enable new disulfide patterns, which could then be selected and fixed in sequence space based on stability and function. As the number of protein folds in nature is thought to be limited, the bovine antibody repertoire may represent a rich

(C) Affinity maturation groups show mutation to and from cysteine. Several groups of clonally related sequences were identified and analyzed for somatic hypermutation. Three groups are shown as examples (labeled 1 to 3 on the left). Sequence differences from cysteine are highlighted in red. The number of times each sequence is represented in the cluster is shown at the right.
See also Figures S1, S2, and S3.

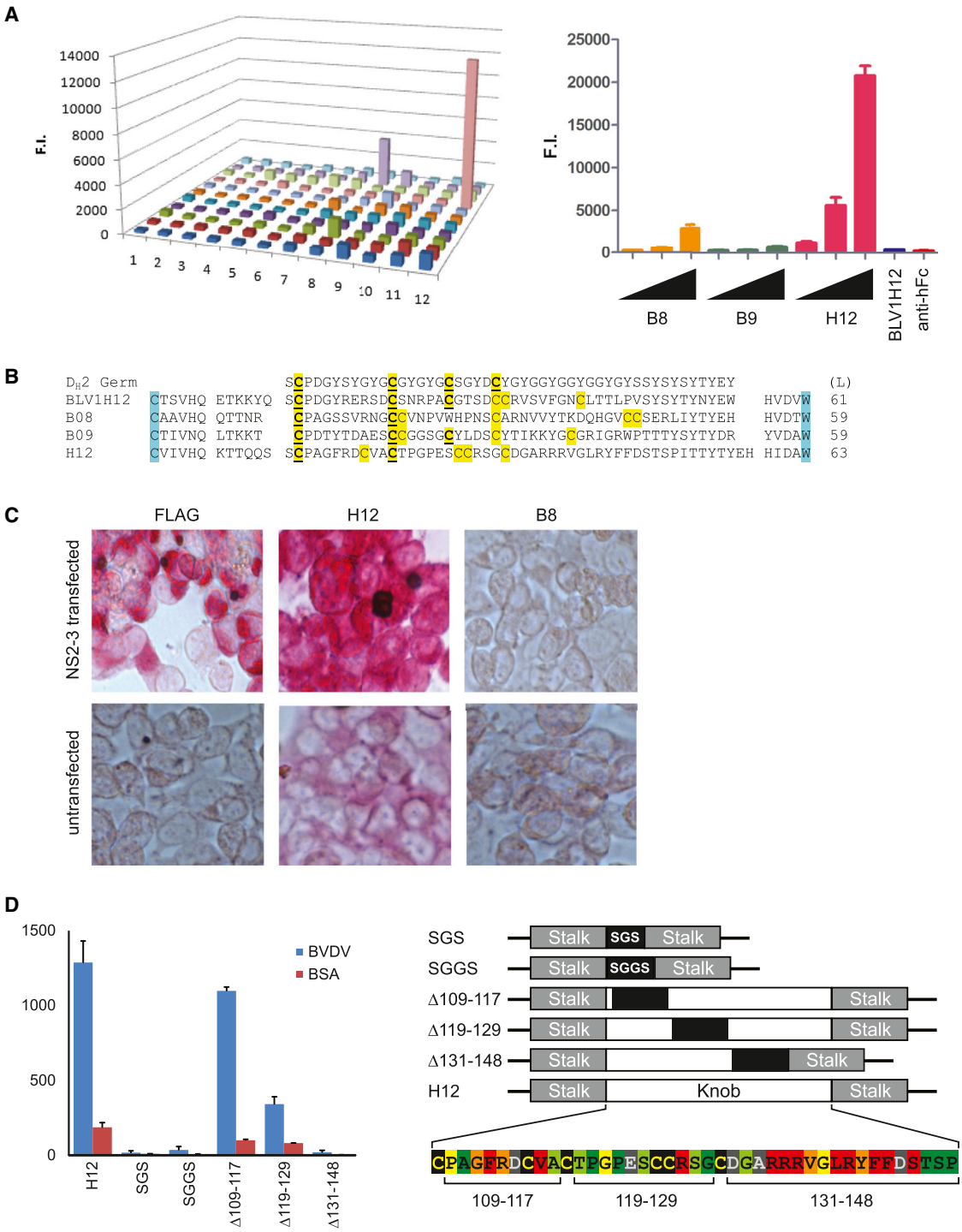

Figure 6. Bovine Antibodies with Ultralong CDR H3s Bind Antigen

(A) ELISA of 132 ultralong CDR H3 antibodies against BVDV (left) and binding activity of the "hits" B8, B9, and H12 in a titration assay (right).

(B) The sequences of B8, H9, and H12 are shown in comparison to BLV1H12 and the germline D_H2 region. Lengths (L) of the CDR H3 are indicated at the right. Cysteines conserved with D_H2 are underlined.

(C) H12 binds NS2-3 on cells. A flag-tagged BVDV NS2-3 protein construct was transfected into HEK293A cells and stained with anti-Flag as a positive control (left), the H12 antibody (middle), and B8 (right). Binding assays with untransfected cells are shown on the bottom.

(D) H12 binding to BVDV requires the knob domain. Binding to BVDV (blue) or BSA (red) was assessed by ELISA for knob mutants of H12. Constructs included a total replacement of the knob sequence with a short linker (SGS or SGGS), partial knob replacements from residues 109–117, 119–129, or 131–148 with an irrelevant sequence (ETYYGSGL). Alanine scan mutants of H12 knob residues were tested for BVDV binding (Figure S4), and the results are summarized in the

(legend continued on next page)

source for discovery of uniquely folded small domains and may provide an unusual opportunity to study protein fold evolution. As antibodies are now a major drug class, with alternative scaffolds such as camelid V_{HH}s becoming more important in biomedicine, the bovine structural diversity paradigm could also find utility in drug or diagnostic discovery through further protein engineering efforts.

The enormous number of unrelated sequences that we found during deep sequencing suggests that diversity on its own is a major functional driver of the ultralong CDR H3 repertoire. It is curious that cattle have this unique structural repertoire in addition to a more conventional shorter CDR H3 repertoire. Physiologically, cattle are unusual in having a rumen, which functions as a ''fermenter'' to metabolize feedstuff. Control of the high titer of natural rumen microorganisms is important to inhibit opportunistic digestive tract or serum infections. The added diversity brought about by this unusual antibody structure could serve this purpose and could perhaps be optimized to bind certain antigens like pores, channels, or other receptors that are more difficult to access with typical antibodies (Figure 7B). The rumen biomass includes a substantial portion of eukaryotic microorganisms, which may present different antigen structures than viruses and bacteria, which are the major challenges for other vertebrate immune systems. Although we could identify ultralong antibodies against BVDV from immunized cattle, the pressure behind the evolution of ''stalk and knob'' features may have been by other unknown antigens not easily targeted by the traditional antibody binding scaffold. Several small disulfide-bonded protein families involved in diverse protein-protein interactions have a general shape and dimension similar to the knob of these bovine antibodies, including protease inhibitors, channel blockers, arthropod toxins, and G-protein-coupled receptor (GPCR) ligands (Figure S5) (Craik et al., 2001; Silverman et al., 2005; Smith et al., 2011). However, no sequence or structural homology could be found with any of these domains and the BLV1H12 or BLV5B8 knobs. Clearly, small disulfide-bonded protein structures have evolved over time for a multitude of protein-protein interactions of diverse function. Indeed, the ''knottin'' family of disulfide-bonded proteins has been engineered for a number of different applications using in vitro display technologies (Gracy and Chiche, 2011; Kolmar, 2009; Moore and Cochran, 2012). The bovine antibody system provides an analogous in vivo process for evolution of these small domains but may also enable unique disulfide pattern diversity and effector functions mediated by the immunoglobulin constant regions.

The propensity for structural and sequence diversity of the stalk and knob motifs could have more general implications. A long stable β ribbon connecting two unrelated domains is rare. Exposed β strands can often initiate protein-protein interactions (Richardson and Richardson, 2002). It is interesting to speculate that the significant diversity of the ascending strand provides a nidus for interaction with some antigens, with the diversity of the knob providing additional high-affinity contacts through affinity maturation. Also, each ultralong CDR H3 knob has several disulfide-produced loops that could interact with antigen, as we have shown for the H12 antibody. Alternatively, positive charges in the knob could also allow membrane binding or penetration, with the stalk acting to bind surface or membrane proteins. The biophysical and detailed binding properties of this new class of antigen receptor require further investigation.

A significant paradox in adaptive immune evolution is the fact that some species utilize a large number of V, D, and J segments, whereas others have a very limited combinatorial repertoire (Figure 7B and Table S6). For cattle, this limited combinatorial repertoire is expanded enormously by the ability to create structural diversity within ultralong CDR H3s on a scaffold encoded by only a single V_HBUL, D_H2, and J_H paired with a limited number of V_λ light chains (Figures 3 and 7 and Table S6). The limitations in V_H and V_L usage may be due to the structural constraints imposed by the stalk interaction with other CDRs. In the same way that substantial diversity can be produced combinatorially by V(D)J recombination in other species, the bovine mechanism of generating cysteine-mediated hypervariable minifolds de novo enables a small amount of germline-encoded genetic material to generate substantial sequence and structural diversity, representing a unique mechanism for immune receptor repertoire generation.

EXPERIMENTAL PROCEDURES

Crystallization and Structure Determination of BLV1H12 and BLV5B8

The bovine Fab fragments were cloned and purified as described in the Extended Experimental Procedures. Gel filtration fractions containing the bovine Fabs were concentrated to ~10 mg/ml in 10 mM Tris (pH 8.0) and 50 mM NaCl. Initial crystallization trials were set up using the automated Rigaku Crystalmation robotic system at the Joint Center for Structural Genomics (http://www.jcsg.org). Several hits were obtained for BLV1H12 and BLV5B8, and crystals used for data collection were grown by the sitting drop vapor diffusion method with a reservoir solution (100 μl) containing 0.27 M potassium citrate and 22% PEG 3350 (BLV1H12) and 0.2 M disodium tartrate and 20% PEG 3350 (BLV5B8). Drops consisting of 100 nl protein + 100 nl precipitant were set up at 20°C, and crystals appeared within 3 to 7 days. The resulting crystals were cryoprotected using well solution supplemented with 15% ethylene glycol then flash cooled and stored in liquid nitrogen until data collection.

Diffraction data were collected on the GM/CA-CAT 23ID-D beamline at the Advanced Photon Source at Argonne National Laboratory (BLV1H12) and the 11-1 beamline at the Stanford Synchrotron Radiation Lightsource for BLV5B8. Both data sets were indexed in spacegroup $P2_12_12_1$, integrated, scaled, and merged using HKL2000 (BLV5B8; HKL Research) or XPREP (BLV1H12; Bruker). The BLV1H12 structure was solved by molecular replacement to 1.85 Å resolution using Phaser (McCoy et al., 2007). Fab variable domains from 1BVK and constant domains from 2FB4 were used as search models, and two complete BLV1H12 Fabs were found in the asymmetric unit. The BLV5B8 data set was also solved by molecular replacement (to 2.20 Å), using the refined BLV1H12 coordinates as a model. Rigid body refinement, simulated annealing, and restrained refinement (including TLS refinement, with one group for each Ig domain and one for each CDR H3) were carried out in Phenix (Adams et al., 2010). Riding hydrogens were used during refinement. Between rounds of refinement, the model was built and adjusted using

colored alignment (lower right). Knob point mutant binding to BVDV was compared to that of unmodified H12 (<20%, red; 20%–40%, orange; 40%–60%, yellow; 60%–80%, light green; >80%, green). Some point mutants had greater than 3-fold higher binding to BSA alone, indicating higher nonspecific interactions (gray, Figure S4). All H12 IgGs were normalized to 30 nM (except as indicated in Figure S4 due to poor expression).
Data are represented as the mean ± SEM. See also Figure S4 and Table S7.

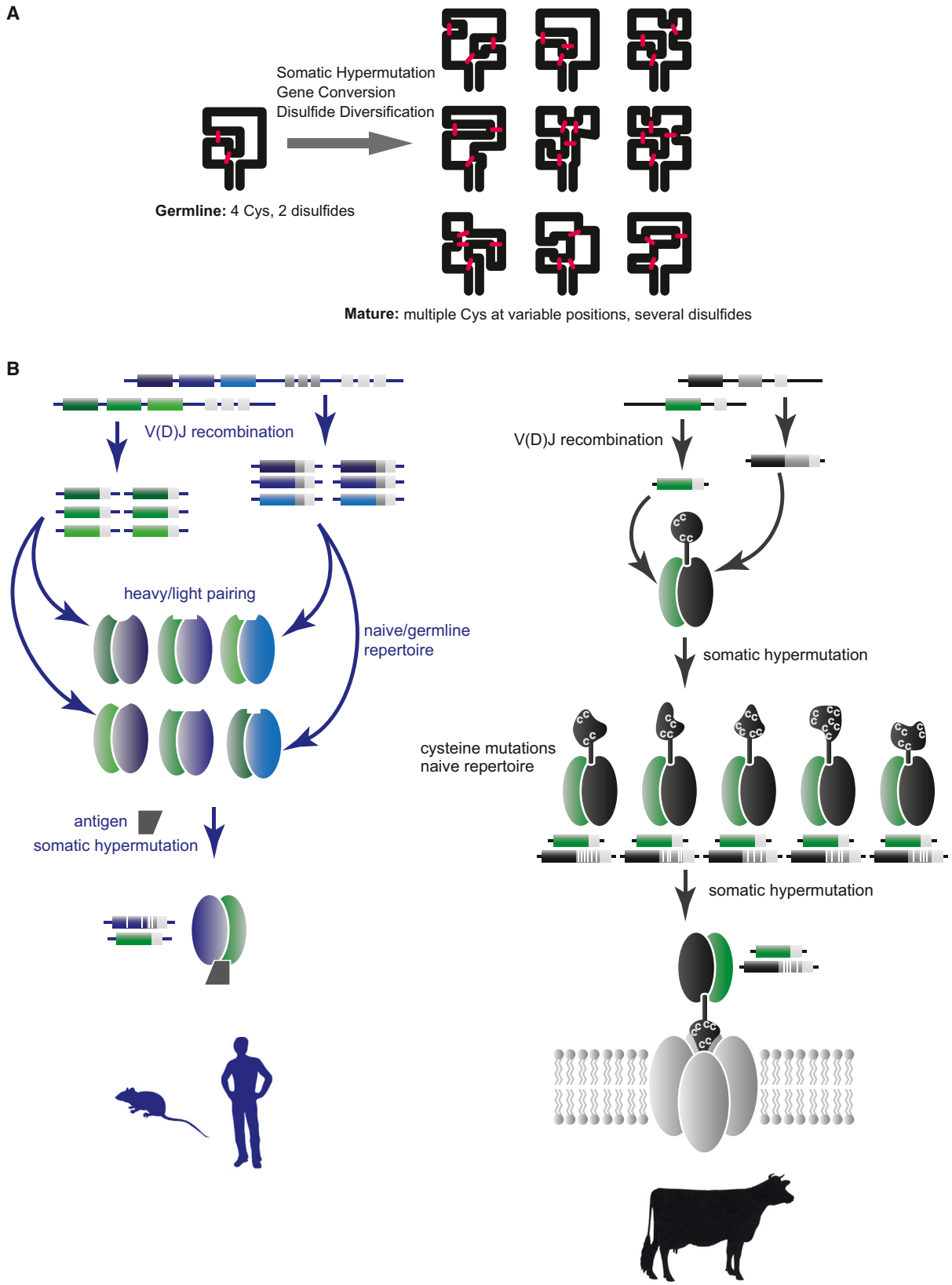

(legend on next page)

Coot (Emsley et al., 2010). Waters were built automatically using the "ordered_solvent" modeling function in Phenix (Adams et al., 2010). Structures were validated using the JCSG QC Server (publicly available at http://smb.slac.stanford.edu/jcsg/QC/), which includes Molprobity (Chen et al., 2010). Refinement statistics can be found in Table S1.

Ultralong cDNA Generation

Bovine spleen and lymph nodes were obtained from Animal Technologies (Tyler, TX), or from Texas A&M University. Total RNA was isolated from bovine tissues using TRIzol reagent (Invitrogen, Carlsbad, CA) following the manufacturer's protocol, followed by on column digestion of DNA using the RNeasy Mini Kit (QIAGEN, Valencia, CA). RNA quantity and quality were assessed with Nanodrop (Thermal Scientific), Qubit RNA, and Agilent 2100 Bioanalyzer (Agilent, Santa Clara, CA), following the manufacturer's protocols. Total RNA was used as a template for complementary DNA (cDNA) synthesis catalyzed by Superscript II (Invitrogen). The antibody variable region was amplified from cDNA using primers 5′-TTGAGCGACAAGGCTGTAGGCTG-3′and 5′-CTTTCGGGGCTGTGGTGGAGGC-3′.

Deep Sequencing

Bar-coded primers (Table S2) were used to amplify V_H from bovine spleen cDNA. The amplicons of V_H were purified from 2% agarose gels and deep sequenced according to Roche 454 GS FLX instructions. Bioinformatic analysis is described in detail in the Extended Experimental Procedures. CDR H3s were defined by the third residue following the conserved cysteine in framework 3 to the residue immediately preceding the conserved tryptophan in framework 4. This cysteine and tryptophan are highlighted cyan in the figures. V_HBUL was identified by BLAST searching the bovine genome (assembly Btau_4.6.1) with multiple ultralong V_H sequences identified by deep sequencing. It is unclear whether V_HBUL is similar to an uncharacterized partial germline sequence g1.110.10, which has been associated with some ultralong antibodies (Koti et al., 2008; Saini et al., 1999).

FISH Analysis

Five sets of primers (Table S3) specific for the V_HBUL region exons and flanking sequence were used to screen superpools and plate-pools of the bovine genomic TAMBET BAC library (Cai et al., 1995) by PCR. Three positive clones, 14-74H6, 318H2, and 7138-19E8 were identified, picked, and grown in 2YT with chloramphenicol. Bacterial artificial chromosome (BAC) DNA was isolated with the Plasmid Midi Kit (QIAGEN) according to the manufacturer's instructions. Physical location of the BACs was determined by fluorescence in situ hybridization (FISH) to cattle metaphase chromosomes as described (Raudsepp and Chowdhary, 2008). Briefly, DNA from individual BAC clones was labeled with biotin-16-dUTP or digoxigenin-11-dUTP, using Biotin- or DIG-Nick Translation Mix (Roche Applied Science), respectively. Differently labeled probes were hybridized in pairs to metaphase chromosomes. Biotin and digoxigenin were detected with avidin-FITC and anti-digoxigenin-Rhodamine, respectively. Images for a minimum of ten metaphase spreads were captured for each experiment and analyzed with a Zeiss Axioplan2 fluorescence microscope equipped with Isis V5.2 (MetaSystems GmbH) software. Cattle chromosomes were counterstained with DAPI and identified according to international nomenclature (Cribiu et al., 2001).

Immunization of Cattle with Whole Killed BVDV

A 4-month-old Holstein steer was immunized by intradermal inoculation of a mixture of heat-killed BVDV-1 and BVDV-2 (100 μg of each). The inactivated virus mixture was suspended in 500 μl PBS and emulsified in 500 μl Freund's complete adjuvant by repeated passage through a double-barrel needle. The immunogen was inoculated intradermally (200 μl/injection) at the neck region using a 26 × 1½ G needle. The steer was boosted three times at monthly intervals with the same amount of antigen but formulated in Freund's incomplete adjuvant. Sero-conversion was tested by ELISA using plates coated with the inactivated virus and by immunocytometric analysis of MDBK cells infected with either BVDV-1 or BVDV-2. The steer was bled from the jugular vein, and blood was collected in heparin. Lymphocytes were purified through Lymphocyte Separation Media (Mediatech) centrifugation and stored in RNAlater.

Anti-BVDV IgG Generation

The V_H (generated as cDNA, described above) was assembled with bovine C_H1 and human IgG1 Fc and ligated into pFUSE expression vector to afford a full-length heavy-chain library. 500 single *E. coli* transformants were picked and sequenced. 132 clones containing unique heavy-chain sequences were selected. The heavy-chain library was then cotransfected with pFUSE expression vector encoding the invariant bovine light chain into HEK293T cells using 293Fectin (Life Technologies) to generate a small spatially addressed library (Mao et al., 2010). Antibodies were secreted into culture media and harvested in 96 well format for further testing. The chimeric antibodies were quantified by sandwich ELISA, screened for binding to BVDV by ELISA, and analyzed for cell binding by immunocytometry as described in the Extended Experimental Procedures.

BDVH12 Knob Mutation Cloning

BsaI restriction sites were engineered into the knob region and used to insert oligonucleotides encoding mutated amino acid residues (Table S7), as described in detail in the Extended Experimental Procedures.

ACCESSION NUMBERS

Crystallographic coordinates and structure factors have been deposited in the Protein Data Bank (PDB) with the following PDB codes: 4K3D (antibody BLV1H12 Fab) and 4K3E (antibody BLV5B8 Fab).

SUPPLEMENTAL INFORMATION

Supplemental Information includes Extended Experimental Procedures, five figures, and seven tables and can be found with this article online at http://dx.doi.org/10.1016/j.cell.2013.04.049.

ACKNOWLEDGMENTS

We thank Richard Lerner, Michael McHeyzer-Williams, Jeffery Kelly, and Michael Weiss for helpful discussions and Cory Bentley, Evan Holmes, James Graziano, Miguel de los Rios, and Jocelyn Bray for technical support. This work was supported by American Cancer Society Grant ACS RSG-09-1601 (to V.V.S.), National Institutes of Health Grants R01GM062159 (to P.G.S.) and R01 AI084817 (to I.A.W.), the Skaggs Institute for Chemical Biology (to P.G.S. and I.A.W.), and the Scripps Translational Sciences Institute Clinical Translational Science Award UL1 RR025774-03 (to A.T.). This is manuscript number 21869 of The Scripps Research Institute. V.V.S. and O.B. have equity interests in Fabrus, Inc. Please contact I.A.W. for structural information and V.V.S. for other inquiries.

Figure 7. Model for Ultralong CDR H3 Diversification into Minifolds

(A) A schematic of the D_H2 knob with four cysteines is shown on the left, with SH and/or gene conversion leading to a multitude of cysteine patterns and loops on the right.

(B) Mechanisms for generating antibody diversity. In humans and mice (left), combinatorial diversity through V(D)J recombination and V_H-V_L pairing creates a multitude of different binding sites, which are further optimized following antigen exposure by somatic hypermutation. In cows (right), combinatorial diversity is severely limited; however, somatic mutation to and from cysteines can reshape the "knob" region, creating substantial structural diversity in ultralong CDR H3s. These antibodies may be further optimized through SH and may bind unique targets such as pores or channels.

See also Figure S5 and Table S6.

Received: October 31, 2012
Revised: February 15, 2013
Accepted: April 23, 2013
Published: June 6, 2013

REFERENCES

Adams, P.D., Afonine, P.V., Bunkóczi, G., Chen, V.B., Davis, I.W., Echols, N., Headd, J.J., Hung, L.W., Kapral, G.J., Grosse-Kunstleve, R.W., et al. (2010). PHENIX: a comprehensive Python-based system for macromolecular structure solution. Acta Crystallogr. D Biol. Crystallogr. *66*, 213–221.

Agapov, E.V., Murray, C.L., Frolov, I., Qu, L., Myers, T.M., and Rice, C.M. (2004). Uncleaved NS2-3 is required for production of infectious bovine viral diarrhea virus. J. Virol. *78*, 2414–2425.

Alder, M.N., Rogozin, I.B., Iyer, L.M., Glazko, G.V., Cooper, M.D., and Pancer, Z. (2005). Diversity and function of adaptive immune receptors in a jawless vertebrate. Science *310*, 1970–1973.

Almagro, J.C., Raghunathan, G., Beil, E., Janecki, D.J., Chen, Q., Dinh, T., LaCombe, A., Connor, J., Ware, M., Kim, P.H., et al. (2012). Characterization of a high-affinity human antibody with a disulfide bridge in the third complementarity-determining region of the heavy chain. J. Mol. Recognit. *25*, 125–135.

Berens, S.J., Wylie, D.E., and Lopez, O.J. (1997). Use of a single VH family and long CDR3s in the variable region of cattle Ig heavy chains. Int. Immunol. *9*, 189–199.

Cai, L., Taylor, J.F., Wing, R.A., Gallagher, D.S., Woo, S.S., and Davis, S.K. (1995). Construction and characterization of a bovine bacterial artificial chromosome library. Genomics *29*, 413–425.

Chen, V.B., Arendall, W.B., 3rd, Headd, J.J., Keedy, D.A., Immormino, R.M., Kapral, G.J., Murray, L.W., Richardson, J.S., and Richardson, D.C. (2010). MolProbity: all-atom structure validation for macromolecular crystallography. Acta Crystallogr. D Biol. Crystallogr. *66*, 12–21.

Collis, A.V.J., Brouwer, A.P., and Martin, A.C.R. (2003). Analysis of the antigen combining site: correlations between length and sequence composition of the hypervariable loops and the nature of the antigen. J. Mol. Biol. *325*, 337–354.

Craik, D.J., Daly, N.L., and Waine, C. (2001). The cystine knot motif in toxins and implications for drug design. Toxicon *39*, 43–60.

Cribiu, E.P., Di Berardino, D., Di Meo, G.P., Eggen, A., Gallagher, D.S., Gustavsson, I., Hayes, H., Iannuzzi, L., Popescu, C.P., Rubes, J., et al. (2001). International System for Chromosome Nomenclature of Domestic Bovids (ISCNDB 2000). Cytogenet. Cell Genet. *92*, 283–299.

Decanniere, K., Desmyter, A., Lauwereys, M., Ghahroudi, M.A., Muyldermans, S., and Wyns, L. (1999). A single-domain antibody fragment in complex with RNase A: non-canonical loop structures and nanomolar affinity using two CDR loops. Structure *7*, 361–370.

Di Noia, J.M., and Neuberger, M.S. (2007). Molecular mechanisms of antibody somatic hypermutation. Annu. Rev. Biochem. *76*, 1–22.

Ekiert, D.C., Kashyap, A.K., Steel, J., Rubrum, A., Bhabha, G., Khayat, R., Lee, J.H., Dillon, M.A., O'Neil, R.E., Faynboym, A.M., et al. (2012). Cross-neutralization of influenza A viruses mediated by a single antibody loop. Nature *489*, 526–532.

Elsik, C.G., Tellam, R.L., Worley, K.C., Gibbs, R.A., Muzny, D.M., Weinstock, G.M., Adelson, D.L., Eichler, E.E., Elnitski, L., Guigó, R., et al.; Bovine Genome Sequencing and Analysis Consortium. (2009). The genome sequence of taurine cattle: a window to ruminant biology and evolution. Science *324*, 522–528.

Emsley, P., Lohkamp, B., Scott, W.G., and Cowtan, K. (2010). Features and development of Coot. Acta Crystallogr. D Biol. Crystallogr. *66*, 486–501.

Fugmann, S.D., Lee, A.I., Shockett, P.E., Villey, I.J., and Schatz, D.G. (2000). The RAG proteins and V(D)J recombination: complexes, ends, and transposition. Annu. Rev. Immunol. *18*, 495–527.

Gracy, J., and Chiche, L. (2011). Structure and modeling of knottins, a promising molecular scaffold for drug discovery. Curr. Pharm. Des. *17*, 4337–4350.

Han, B.W., Herrin, B.R., Cooper, M.D., and Wilson, I.A. (2008). Antigen recognition by variable lymphocyte receptors. Science *321*, 1834–1837.

Hosseini, A., Campbell, G., Prorocic, M., and Aitken, R. (2004). Duplicated copies of the bovine JH locus contribute to the Ig repertoire. Int. Immunol. *16*, 843–852.

Kato, L., Stanlie, A., Begum, N.A., Kobayashi, M., Aida, M., and Honjo, T. (2012). An evolutionary view of the mechanism for immune and genome diversity. J. Immunol. *188*, 3559–3566.

Kocks, C., and Rajewsky, K. (1988). Stepwise intraclonal maturation of antibody affinity through somatic hypermutation. Proc. Natl. Acad. Sci. USA *85*, 8206–8210.

Kolmar, H. (2009). Biological diversity and therapeutic potential of natural and engineered cystine knot miniproteins. Curr. Opin. Pharmacol. *9*, 608–614.

Koti, M., Kataeva, G., and Kaushik, A. (2008). Organization of D(H)-gene locus is distinct in cattle. Dev. Biol. (Basel) *132*, 307–313.

Koti, M., Kataeva, G., and Kaushik, A.K. (2010). Novel atypical nucleotide insertions specifically at VH-DH junction generate exceptionally long CDR3H in cattle antibodies. Mol. Immunol. *47*, 2119–2128.

Kwong, P.D., and Wilson, I.A. (2009). HIV-1 and influenza antibodies: seeing antigens in new ways. Nat. Immunol. *10*, 573–578.

Lopez, O., Perez, C., and Wylie, D. (1998). A single VH family and long CDR3s are the targets for hypermutation in bovine immunoglobulin heavy chains. Immunol. Rev. *162*, 55–66.

Mao, H., Graziano, J.J., Chase, T.M., Bentley, C.A., Bazirgan, O.A., Reddy, N.P., Song, B.D., and Smider, V.V. (2010). Spatially addressed combinatorial protein libraries for recombinant antibody discovery and optimization. Nat. Biotechnol. *28*, 1195–1202.

McLellan, J.S., Pancera, M., Carrico, C., Gorman, J., Julien, J.P., Khayat, R., Louder, R., Pejchal, R., Sastry, M., Dai, K., et al. (2011). Structure of HIV-1 gp120 V1/V2 domain with broadly neutralizing antibody PG9. Nature *480*, 336–343.

McCoy, A.J., Grosse-Kunstleve, R.W., Adams, P.D., Winn, M.D., Storoni, L.C., and Read, R.J. (2007). Phaser crystallographic software. J. Appl. Cryst. *40*, 658–674.

Moore, S.J., and Cochran, J.R. (2012). Engineering Knottins as Novel Binding Agents. In Methods in Enzymology, K.D. Wittrup and L.V. Gregory, eds. (San Diego: Academic Press), pp. 223–251.

Njongmeta, L.M., Bray, J., Davies, C.J., Davis, W.C., Howard, C.J., Hope, J.C., Palmer, G.H., Brown, W.C., and Mwangi, W. (2012). CD205 antigen targeting combined with dendritic cell recruitment factors and antigen-linked CD40L activation primes and expands significant antigen-specific antibody and CD4(+) T cell responses following DNA vaccination of outbred animals. Vaccine *30*, 1624–1635.

Pancer, Z., Amemiya, C.T., Ehrhardt, G.R., Ceitlin, J., Gartland, G.L., and Cooper, M.D. (2004). Somatic diversification of variable lymphocyte receptors in the agnathan sea lamprey. Nature *430*, 174–180.

Parng, C.L., Hansal, S., Goldsby, R.A., and Osborne, B.A. (1996). Gene conversion contributes to Ig light chain diversity in cattle. J. Immunol. *157*, 5478–5486.

Pejchal, R., Walker, L.M., Stanfield, R.L., Phogat, S.K., Koff, W.C., Poignard, P., Burton, D.R., and Wilson, I.A. (2010). Structure and function of broadly reactive antibody PG16 reveal an H3 subdomain that mediates potent neutralization of HIV-1. Proc. Natl. Acad. Sci. USA *107*, 11483–11488.

Raudsepp, T., and Chowdhary, B.P. (2008). FISH for mapping single copy genes. Methods Mol. Biol. *422*, 31–49.

Richardson, J.S., and Richardson, D.C. (2002). Natural β-sheet proteins use negative design to avoid edge-to-edge aggregation. Proc. Natl. Acad. Sci. USA *99*, 2754–2759.

Saini, S.S., Allore, B., Jacobs, R.M., and Kaushik, A. (1999). Exceptionally long CDR3H region with multiple cysteine residues in functional bovine IgM antibodies. Eur. J. Immunol. *29*, 2420–2426.

Saini, S.S., Farrugia, W., Ramsland, P.A., and Kaushik, A.K. (2003). Bovine IgM antibodies with exceptionally long complementarity-determining region 3 of the heavy chain share unique structural properties conferring restricted VH + Vlambda pairings. Int. Immunol. *15*, 845–853.

Saphire, E.O., Parren, P.W.H.I., Pantophlet, R., Zwick, M.B., Morris, G.M., Rudd, P.M., Dwek, R.A., Stanfield, R.L., Burton, D.R., and Wilson, I.A. (2001). Crystal structure of a neutralizing human IGG against HIV-1: a template for vaccine design. Science *293*, 1155–1159.

Silverman, J., Liu, Q., Bakker, A., To, W., Duguay, A., Alba, B.M., Smith, R., Rivas, A., Li, P., Le, H., et al. (2005). Multivalent avimer proteins evolved by exon shuffling of a family of human receptor domains. Nat. Biotechnol. *23*, 1556–1561.

Sinclair, M.C., Gilchrist, J., and Aitken, R. (1997). Bovine IgG repertoire is dominated by a single diversified VH gene family. J. Immunol. *159*, 3883–3889.

Smider, V., and Chu, G. (1997). The end-joining reaction in V(D)J recombination. Semin. Immunol. *9*, 189–197.

Smith, J.J., Hill, J.M., Little, M.J., Nicholson, G.M., King, G.F., and Alewood, P.F. (2011). Unique scorpion toxin with a putative ancestral fold provides insight into evolution of the inhibitor cystine knot motif. Proc. Natl. Acad. Sci. USA *108*, 10478–10483.

Stanfield, R.L., Dooley, H., Flajnik, M.F., and Wilson, I.A. (2004). Crystal structure of a shark single-domain antibody V region in complex with lysozyme. Science *305*, 1770–1773.

Thomson, C.A., Bryson, S., McLean, G.R., Creagh, A.L., Pai, E.F., and Schrader, J.W. (2008). Germline V-genes sculpt the binding site of a family of antibodies neutralizing human cytomegalovirus. EMBO J. *27*, 2592–2602.

Wang, F., Sen, S., Zhang, Y., Ahmad, I., Zhu, X., Wilson, I.A., Smider, V.V., Magliery, T.J., and Schultz, P.G. (2013). Somatic hypermutation maintains antibody thermodynamic stability during affinity maturation. Proc. Natl. Acad. Sci. USA *110*, 4261–4266.

Zhao, Y., Jackson, S.M., and Aitken, R. (2006). The bovine antibody repertoire. Dev. Comp. Immunol. *30*, 175–186.

EXTENDED EXPERIMENTAL PROCEDURES

Cloning, Expression, and Purification of Bovine Fabs

Genes encoding the heavy and light chain Fab regions of BLV1H12 and BLV5B8 were generated by gene synthesis (GenScript, Piscataway, NJ). A DNA fragment derived from the promoter region of pFastBacDual (Invitrogen) was fused to the gp67 and the honey bee mellitin (HBM) signal peptides by overlap PCR, yielding a fragment with head-to-head p10 and polyhedrin promoters upstream of the HBM and gp67 signal peptides, respectively (i.e., HBM-p10-pPolyH-gp67). Bovine Fab heavy and light chain regions were fused to the promoter-signal peptide cassette by overlap PCR (heavy chain downstream of pPolyH-gp67 and light chain downstream of p10-HBM), and ligated into the SfiI sites of pDCE361, a derivative of pFastBacDual. A His_6-tag was introduced at the C terminus of the heavy chain to facilitate purification. The resulting baculovirus transfer vectors were used to generate recombinant bacmids using the Bac-to-Bac system (Invitrogen) and virus was rescued by transfecting purified bacmid DNA into Sf9 cells using Cellfectin II (Invitrogen). Both Fab proteins were produced by infecting suspension cultures of Sf9 cells with recombinant baculovirus at an MOI of 5-10 and incubating at 28°C with shaking at 110 RPM. After 72 hr, the cultures were clarified by two rounds of centrifugation at 2,000 g and 10,000 g at 4°C. The supernatant, containing secreted, soluble Fab was concentrated and buffer exchanged into 1x PBS, pH 7.4. After metal affinity chromatography using Ni-NTA resin, Fabs were purified by protein G affinity chromatography (GE Healthcare), cation exchange chromatography (MonoS, GE healthcare), and gel filtration (Superdex200, GE Healthcare).

Sequencing Analysis

Homology Analysis of Ultralong CDR H3s to D_H2

To determine whether the long CDR H3 sequences were derived from the long bovine germline D_H2 gene, we first generated multiple alignments of the unique CDR H3 nucleotide sequences observed in the samples, using MUSCLE (Edgar, 2004). The frequency of each nucleotide, or gap, from these alignments is visualized in Figures S2A–S2C. As can be observed in these plots, all alignments contained anchors of positions with high nucleotide identity, separated by gaps in many of the long CDR H3 sequences. This suggests, with the hypothesis that the long CDR H3 sequences are derived from the bovine germline D_H2 gene, that the high nucleotide identity positions are derived from the germline D sequence, and are separated by nucleotide insertions or deletions specific to individual, or subsets, of the long CDR H3 sequences. Therefore, we generated an ungapped consensus sequence from each sample by simply assigning the most abundant nucleotide, or gap, to each position, and retaining only those positions that were assigned a nucleotide identity. This procedure should eliminate those positions that are due to nucleotide insertions in smaller subsets of the long CDR H3 sequences, as well as those positions that are subject to high diversification during the generation of the final processed long CDR H3. The retained positions should represent germline D-gene derived sequence. The frequency of each nucleotide and/or gap at each position retained in the ungapped consensus sequence is plotted in Figures S2D–S2F. As can be observed in these plots, these positions displayed very high nucleotide identity across the unique long CDR H3 sequences, with an average of ~83% of the long CDR H3 sequences sharing the consensus nucleotide at each position. Consistency across the alignments was even higher in the 5′ and 3′ ends of the alignment, consistent with the expected pattern given the hypothesis that each sequence is derived from processing of the germline D-gene. To formally confirm these positions are, in fact, derived from germline D_H2, we then aligned each ungapped consensus with the germline D-gene, using a Smith-Waterman algorithm, and observed a highly significant match of each consensus sequence to the germline D-gene (72%–75% identity). The correspondence of each ungapped consensus with the germline D-gene can be seen in the multiple alignment presented in Figure 5A. Each consensus ungapped sequence consists of a long block of perfect matches to the conserved flanking portions of the germline D-gene and a central region with blocks of agreement with the germline D-gene sequence separated by gaps of missing nucleotides in the consensus sequences. These gaps suggest there are hotspots where variability is induced in the long CDR H3 antibodies. Overall, we were able to almost fully reconstruct the long germline D-gene sequence from the long CDR H3 reads, confirming that the long CDR H3 sequences do in fact derive from use of D_H2 or a highly related sequence.

Alignment Methods

Multiple alignments were performed with the MUSCLE algorithm (Edgar, 2004). MUSCLE was executed to generate multiple long CDR H3 nucleotide alignments with relatively high gap open (−20.0) and gap extend (−10.0) penalties due to the large amount of heterogeneity observed in the sequences. Local alignment was executed using the Smith-Waterman algorithm with the following settings, match score = 2.0, mismatch penalty = −1.0, gap opening penalty = −2.0, and gap extension penalty = −0.5.

Phylogenetic Tree Generation

Antibody amino acid sequences were aligned using MUSCLE (Edgar, 2004) with a gap-open penalty of −50.0, a gap-extend penalty of −1.0 and default settings otherwise. Multiple instances were included for amino acid sequences represented by multiple nucleotide sequences. The resultant alignments were used to generate phylogenetic trees using the minimum evolution method under the maximum composite likelihood model implemented in MEGA 5.1 (Tamura et al., 2011). Trees were visualized in FigTree (http://tree.bio.ed.ac.uk/software/figtree/).

Cloning Knob Mutations

Sequence encoding BVDV-H12 IgG was modified by overlap PCR to remove BsaI sites from the IgG coding region (oligo 701-704). Then, a directional cloning cassette of sequence 5′- gagacctactatggttcgggtctc-3′ was introduced by overlap PCR to replace the

BDVH12 knob (oligo 705-706). This cassette encodes amino acids ETYYGSGL in frame. The cassette was replaced by BsaI digestion and insertion of annealed oligos to replace the knob sequence with SerGlySer (oligo 707-708) to make H12-SGS, or SerGlyGlySer (709-710) to make H12-SGGS. Larger oligo pairs were similarly annealed and inserted into the cloning cassette to replace the H12 knob with modified knobs that have insertion of the cloning cassette between knob cysteines 1 and 3 (oligos 711-712) producing H12-Δ109-117, between knob cysteines 3 and 6 (oligos 713-714) producing H12-Δ119-129, or knob cysteine 6 and the end of the knob (oligos 715-716) producing H12-Δ131-148 (Table S7). These cassette insertions into a portion of the knob allowed further replacement of the cassette with annealed oligo pairs, each encoding a single point mutation in the knob sequence, to evaluate the role of each knob residue in binding to H12 (Table S7). All knob mutation heavy chains were transfected and expressed in the manner described for the library of cow IgGs from which H12 was discovered.

Antibody Quantification Sandwich ELISA

Anti-human IgG (Sigma-Aldrich) was diluted 1:1000 in PBS and 20ul (40ng) was coated onto Maxisorp plates (Thermo Scientific Nunc). Wells were blocked for 1 hr with TBST +10% Horse serum (Cat# 16050, GIBCO Invitrogen), then washed 4x with TBST. Cell culture supernatants containing secreted IgGs were diluted 1:2500 in TBST+ 10% Horse serum. Diluted supernatants (20ul) were added to each well, incubated at room temperature for 1 hr, and washed 4x with TBST. Goat anti-Bovine H^+L biotin conjugate (Fitzgerald) was diluted 1:3000 in block and 20ul (7ng) were added to each well, incubated for 1 hr, then washed 4x with TBST. Streptavidin-HRP conjugate (RPN1231VS, GE Healthcare) was diluted 1:3000 in block and 20ul were added per well, incubated 1 hr, then washed 4x with TBST. 25ul of TMB HRP substrate (BioFX) was added per well, and incubated at room temperature for 1 min before addition of 25ul 0.6N H_2SO_4 per well. Absorbance at 450nm was measured for each well using a TECAN GENios plate reader. Absorbance of IgG supernatant samples expressing BDVH12 or knob mutations were quantified using a standard curve of BDVH12 IgG of known concentrations.

BVDV ELISA

Killed BVDV (0.2 μg) in 100 μl DPBS was coated on 96-well MaxiSorp ELISA plates (Nunc) for 1 hr at 37°C. The plates were blocked with 200 μl 3% BSA solution in DPBST, (Dulbecco's phosphate buffered saline, 0.25% Tween 20) for 1 hr at 37°C. Samples were incubated with 3% BSA in DPBST for 1 hr at 37°C. Wells were washed 5 times with 200 μl DPBST. Subsequently, Goat Anti-Human IgG (Fc) – HRP conjugated antibody (KPL Inc.) was added at a 1:1,000 dilution in blocking solution and incubated for 1 hr at 37°C. Wells were then washed 10 times with 200 μl DPBST. A 100 μl working solution of QuantaBlu (Pierce) was added to each well and incubated for 5 min at room temperature before plates were read in a SpectraMax M5 plate reader at ex325/em420 nm.

Immunocytometry

Binding of the chimeric recombinant antibodies to BVDV antigens was evaluated by immunocytometric analysis of transfected human embryonic kidney (HEK) 293A cells (Invitrogen), as previously described (Njongmeta et al., 2012). Briefly, HEK293A monolayers grown in 6-well tissue culture plates were transfected with 2 μg/well of plasmid (pCDNA3.3, Invitrogen) encoding BVDV antigens (N^{pro}, E2, or non-structural proteins NS2-3) using Lipofectamine 2000 reagent (Invitrogen), and incubated for 48 hr at 37°C with 5% CO_2. The monolayers were fixed with ice-cold 100% methanol for 10 min, rinsed with PBS, and after blocking for 1 hr with PBS containing 5% fetal bovine serum (blocking buffer), the monolayers were incubated at room temperature for 1 hr with 10 μg/ml of a mouse anti-FLAG M2-alkaline phosphatase (AP)-conjugate (Sigma) in blocking buffer or 10 μg/ml of the chimeric recombinant antibodies (H12 or B8). Monolayers transfected with empty vector were similarly reacted to serve as negative controls and, following washes in blocking buffer, the monolayers probed with the chimeric recombinant antibodies were incubated with a 1/200 dilution of AP-conjugated goat anti-Human IgG (Fc specific) mAb (Sigma) in blocking buffer for 1 hr. Following washes in blocking buffer, the AP activity in all the wells was detected using Fast Red AS-MX substrate (Sigma). Stained cells were visualized and photographed using an IS70 inverted optical microscope (Olympus, Japan) equipped with a camera.

SUPPLEMENTAL REFERENCES

Edgar, R.C. (2004). MUSCLE: multiple sequence alignment with high accuracy and high throughput. Nucleic Acids Res. *32*, 1792–1797.

Tamura, K., Peterson, D., Peterson, N., Stecher, G., Nei, M., and Kumar, S. (2011). MEGA5: molecular evolutionary genetics analysis using maximum likelihood, evolutionary distance, and maximum parsimony methods. Mol. Biol. Evol. *28*, 2731–2739.

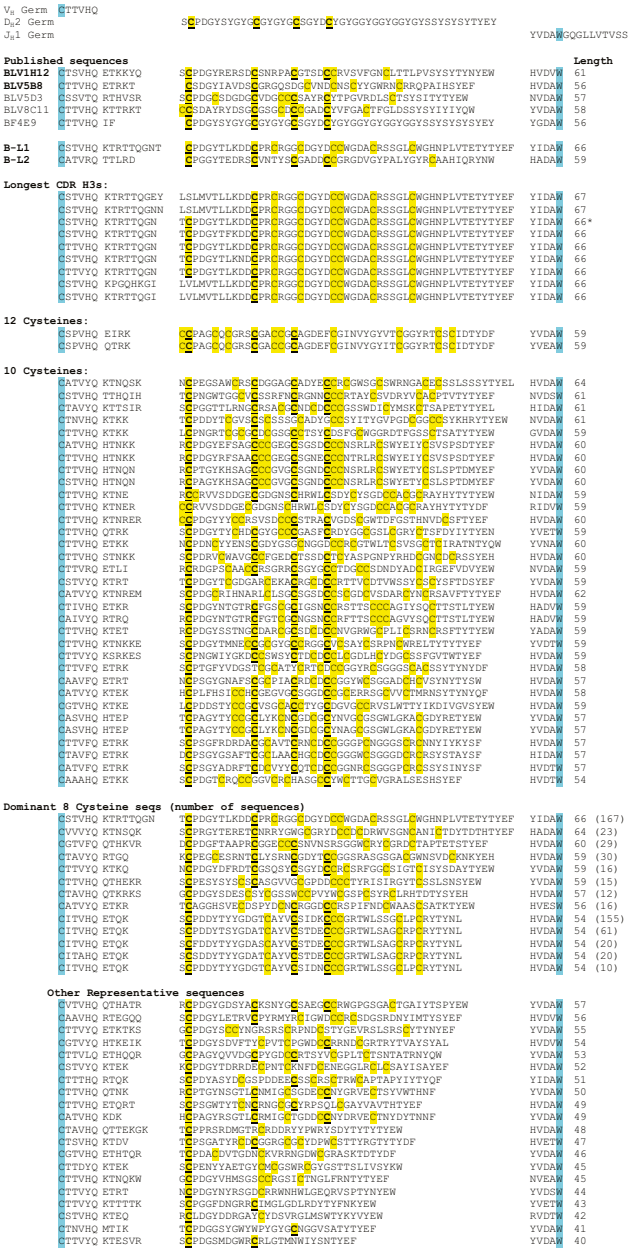

Figure S1. Ultralong Sequences, Related to Figures 1 and 4

(Top) Translation from the germline V_HBUL, D_H2, and J_H. The 5 full length ultralong CDR H3s reported in the literature contain between four and eight cysteines and are not highly homologous to one another; however, some conservation of cysteine residues with D_H2 could be found when the first cysteine of these CDR H3s was "fixed" prior to alignment. Four of the seven sequences (BLV1H12, BLV5D3, BLV8C11, and BF4E9) contain four cysteines in the same positions as D_H2, but also have additional cysteines. BLV5B8 has two cysteines in common with the germline D_H2. This limited homology with some cysteine conservation suggests that mutation of D_H2 could generate these sequences. B-L1 and B-L2 are from our initial sequences from bovine spleen, and the remaining are selected ultralong CDR H3 sequences from deep sequencing data. The first group contains the longest CDR H3s identified to date, and appear clonally related. The * indicates a sequence represented 167 times, suggesting it was strongly selected for function. Several of the eight-cysteine sequences appear selected for function as they were represented multiple times, indicated in parentheses. Other representative sequences of various lengths are indicated in the last group. The framework cysteine and tryptophan residues that define the CDR H3 boundaries are highlighted in cyan. Other cysteines are in yellow, and those conserved with D_H2 are underlined.

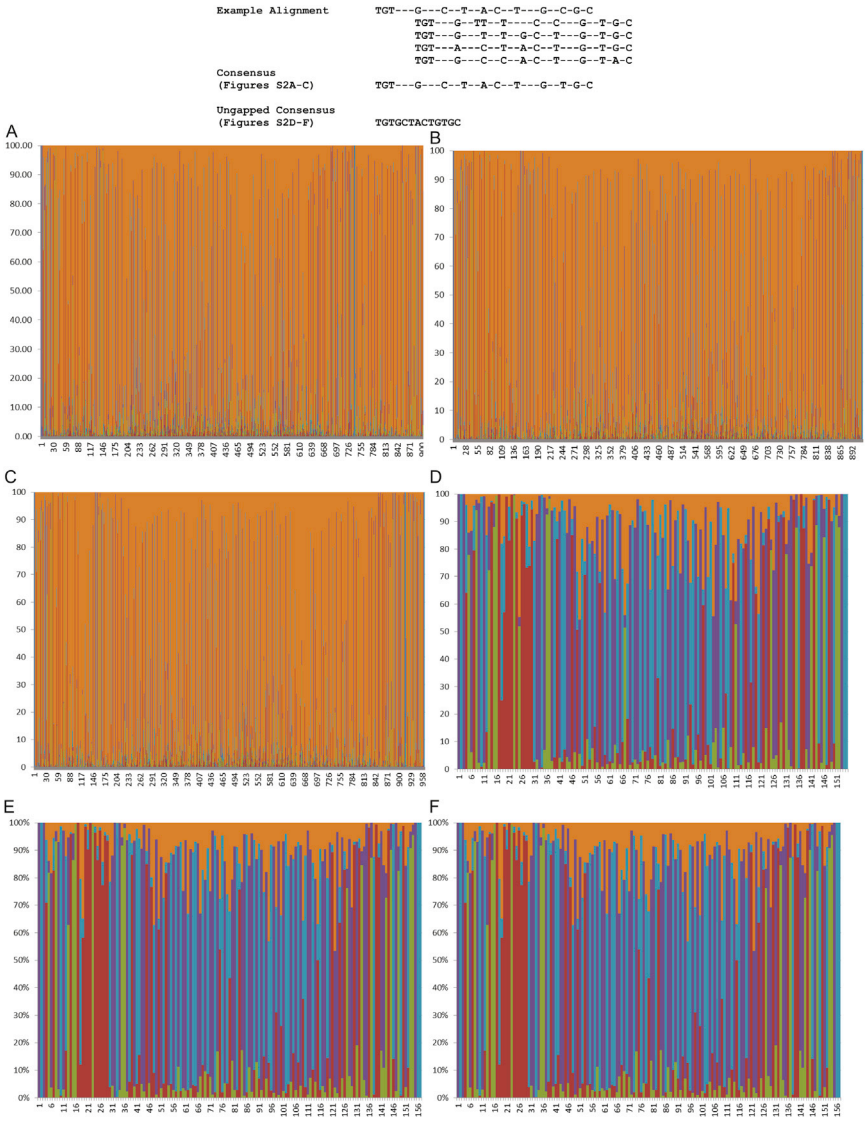

Figure S2. Frequencies of Nucleotides at Each CDR H3 Position, Related to Figure 5

(Top) An example of a gapped alignment and consensus versus the ungapped consensus for a small portion of four sequences.

(A) Frequency of each nucleotide or gap in the consensus alignment of SAMPLE MID10. Red = Adenine, Green = Cytosine, Purple = Thymine, Blue = Guanine, Orange = "Gap." The substantial amount of "gap" (orange) is due to the fact that the ultralong sequences are different lengths, and a proportion of the sequences have insertions or deletions at variable positions. Despite this, regions of very high identity are observed which are separated by gaps, suggesting homology between the ultralong sequences in the context of insertion or deletion events. This plot can be compared to Figure S2D, the ungapped alignment. For details, see the sequence analysis procedures described below.

(B) Frequency of each nucleotide or gap in the consensus alignment of SAMPLE MID11. Red = Adenine, Green = Cytosine, Purple = Thymine, Blue = Guanine, Orange = "Gap."

(C) Frequency of each nucleotide or gap in the consensus alignment of SAMPLE MID1. Red = Adenine, Green = Cytosine, Purple = Thymine, Blue = Guanine, Orange = "Gap."

(D) Frequency of each nucleotide or gap in the ungapped consensus of SAMPLE MID10. Red = Adenine, Green = Cytosine, Purple = Thymine, Blue = Guanine, Orange = "Gap."

(E) Frequency of each nucleotide or gap in the ungapped consensus of SAMPLE MID11. Red = Adenine, Green = Cytosine, Purple = Thymine, Blue = Guanine, Orange = "Gap."

(F) Frequency of each nucleotide or gap in the ungapped consensus of SAMPLE MID1. Red = Adenine, Green = Cytosine, Purple = Thymine, Blue = Guanine, Orange = "Gap."

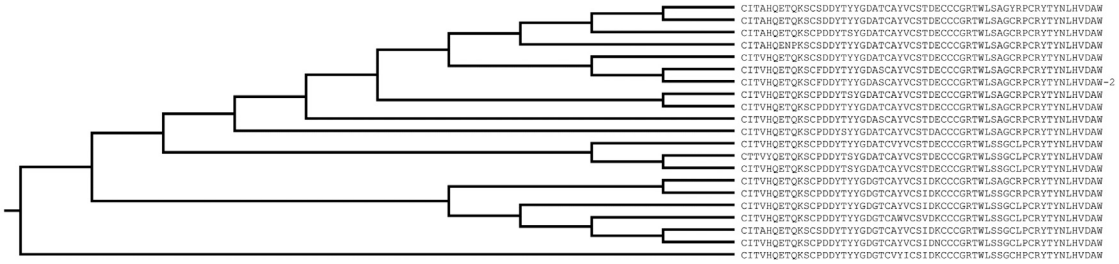

Figure S3. Phylogenetic Tree of Somatically Hypermutated Ultralong CDR H3s, Related to Figure 5

Sequence group #2 from Figure 5C is shown with their evolutionary relationships. The sequence labeled "-2" represents two different nucleotide sequence that translated to the same amino acid sequence.

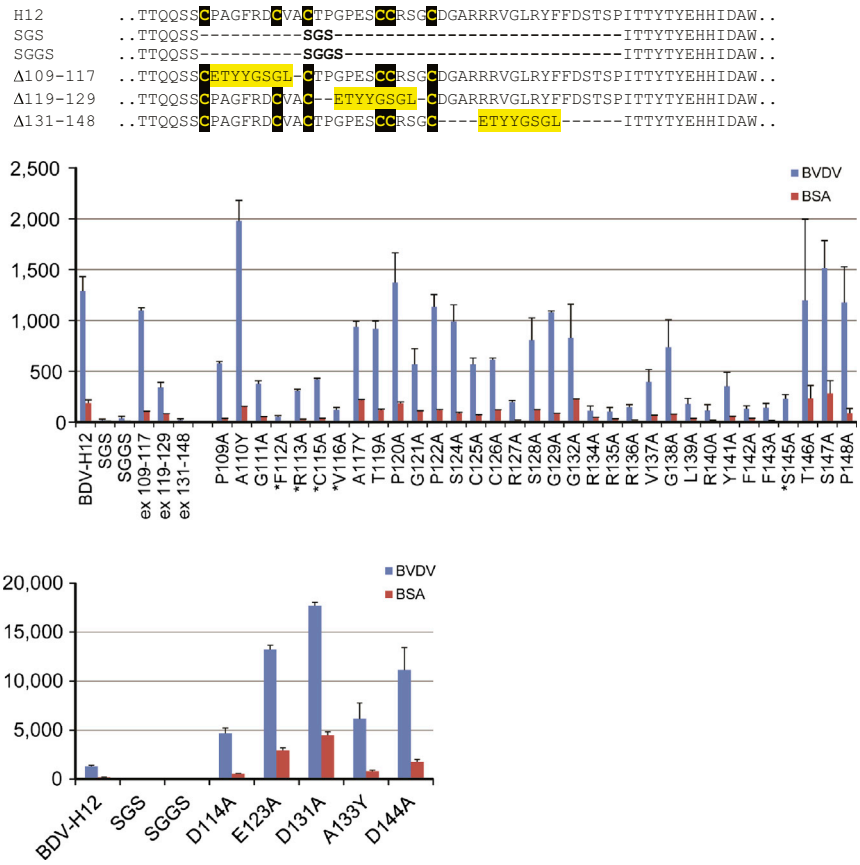

Figure S4. ELISA of H12 "Knob" Mutants, Related to Figure 6

(Top) Peptide sequences of replacement mutants. (Middle) ELISA signals for the knob replacements (left) or point mutations (right). Samples were run in duplicate at 30 nM against BVDV or a BSA negative control. Asterisks indicate point mutations whose expression level did not exceed 30 nM in cell culture supernatants. (Bottom). Non-specific binding mutants. Five point mutants gave abnormally high signals on both BVDV and BSA, indicating these positions may have generally disrupted folding and resulted in non-specific binding activity against BVDV and BSA. The viral particle may have enhanced nonspecific binding due to the greater complexity of the viral surface. Data are represented as the mean +/− SEM.

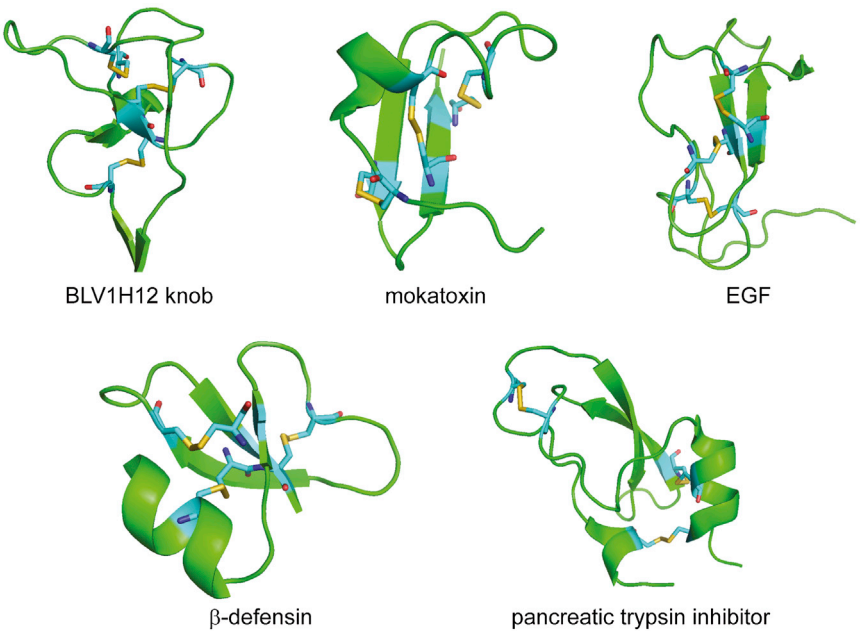

Figure S5. Structures of Several Disulfide-Rich Small Proteins of the Same General Size and Dimensions of the Bovine Ultralong CDR H3 Knob, Related to Figure 7

The BLV1H12 knob is on the left.

Table S1. Data Collection and Refinement Statistics, Related to Figures 1 and 2

Data collection	BLV1H12 Fab	BLV5B8 Fab
Beamline	APS 23ID-D	SSRL 11-1
Wavelength (Å)	1.033	0.979
Space group	$P2_12_12_1$	$P2_12_12_1$
Unit cell parameters (Å, °)	a=71.4, b=127.6, c=127.9, α=β=γ=90	a=54.6, b=53.7, c=330.5, α=β=γ=90
Resolution (Å)	50-1.85 (1.94-1.85)	50-2.20 (2.28-2.20)
Observations	657,691	313,175
Unique Reflections	100,271	49,527
Redundancy	6.5 (4.5)	6.3 (3.5)
Completeness (%)	98.2 (92.3)	96.7 (75.4)
$<I/\sigma_I>$	21.5 (2.5)	17.8 (2.3)
R_{sym}[b]	0.09 (0.73)	0.10 (0.45)
Z_a[c]	2	2
Refinement statistics		
Resolution (Å)	50-1.85 (1.94-1.85)[a]	50-2.20
Reflections (work)	93,312	46,728
Refections (test)	4,921	2,525
R_{cryst}(%)[d] / R_{free}(%)[e]	18.2 / 21.0	20.2 / 24.0
Average B (Å^2)	48.8	45.1
Wilson B (Å^2)	31.9	36.2
Protein atoms	7,061	7,143
Waters	747	507
Other	14	10
RMSD from ideal geometry		
Bond length (Å)	0.008	0.004
Bond angles (°)	1.14	0.95
Ramachandran statistics (%)[f]		
Favored	96.5	96.3
Outliers	0.3	0.1
PDB Code	4K3D	4K3E

[a]Numbers in parentheses refer to the highest resolution shell.
[b]$R_{sym} = \Sigma_{hkl}\Sigma_i \mid I_{hkl,i} - <I_{hkl}> \mid / \Sigma_{hkl}\Sigma_i I_{hkl,I}$ and $R_{pim} = \Sigma_{hkl} (1/(n\text{-}1))^{1/2}\Sigma_i \mid I_{hkl,i} - <I_{hkl}> \mid / \Sigma_{hkl}\Sigma_i I_{hkl,I}$, where $I_{hkl,i}$ is the scaled intensity of the i^{th} measurement of relection h, k, l, $<I_{hkl}>$ is the average intensity for that reflection, and n is the redundancy (Emsley et al., 2010).
[c]Z_a is the number of Fabs per crystallographic asymmetric unit.
[d]$R_{cryst} = \Sigma_{hkl} \mid F_o - F_c \mid / \Sigma_{hkl} \mid F_o \mid$ x 100
[e]R_{free} was calculated as for R_{cryst}, but on a test set comprising 5% of the data excluded from refinement.
[f]Calculated using Molprobity (Chen et al., 2010).

Table S2. Bar-Coded Primers for Deep Sequencing, Related to Figure 4

Primer #	Isotype	Primers
MID1 FW	IgG	CCTATCCCCTGTGTGCCTTGGCAGTCTCAGACGAGTGCGTTTGAGCGACAAGGCTGTAGGCTG
MID1 RV	IgG	CCATCTCATCCCTGCGTGTCTCCGACTCAGACGAGTGCGTCTTTCGGGGCTGTGGTGGAGGC
MID10 FW	IgM	CCTATCCCCTGTGTGCCTTGGCAGTCTCAGTCTCTATGCGTTGAGCGACAAGGCTGTAGGCTG
MID10 RV	IgM	CCATCTCATCCCTGCGTGTCTCCGACTCAGTCTCTATGCGAGTGAAGACTCTCGGGTGTGATTCAC
MID11 FW	IgM	CCTATCCCCTGTGTGCCTTGGCAGTCTCAGTGATACGTCTTTGAGCGACAAGGCTGTAGGCTG
MID11 RV	IgM	CCATCTCATCCCTGCGTGTCTCCGACTCAGTGATACGTCTAGTGAAGACTCTCGGGTGTGATTCAC

Table S3. Summary of Deep Sequencing Results from Bovine Spleen, Related to Figure 4

Source (Bar code)	Cow#1 (MID1)	Cow#1 (MID10)	Cow#2 (MID11)
Ig Class	IgG	IgM	IgM
CDR H3 length range	44-66	44-68	44-69
Number of unique cysteine patterns	655	449	847
Total number of unique long CDR H3 sequences	5633	1639	4456

Table S4: Primers for FISH Analysis, Related to Figure 3

MFC305/Bovine Long VH-F1	5' TTGAGGGACAAGGCTGTAGGCTG 3'
MFC306/Bovine Long VH-R1	5' CTGGTGCACAGTAGTACAGTAGTATGTGG 3'
MFC308/Bovine Long CDR3 Locus F1	5' CTAAGGAGCTCCCAGGAGCTGTC 3'
MFC309/Bovine Long CDR3 Locus R1	5' CTGTGAACACAGTAGACATTTGTGCTG 3'
MFC310/Bovine Long CDR3 Locus F2	5' AGGGGTCCCCAGTGCTGCATATG 3'
MFC311/Bovine Long CDR3 Locus R2	5' TTGAGGCGAGATGGTATCACCCTG 3'
MFC315/Bovine Long CDR3 Locus F3	5' CAGCACAAATGTCTACTGTGTTCACAG 3'
MFC316/Bovine Long CDR3 Locus R3	5' CACCACACATTCAGGTACCAGCC 3'
MFC317/Bovine Long CDR3 Locus F4	5' CCCTCTTCTGTGTCCTGGTAATTCC 3'
MFC318/Bovine Long CDR3 Locus R4	5' ATATGCAGCACTGGGGACCCCTG 3'

Table S5. Bovine Ultralong CDR H3s Have Diverse Cysteine Patterns, Related to Figure 4

Cysteine pattern (MID1)	Abundance (%)
$CX_{10}CX_5CX_5CXCX_7C$	10.44%
$CX_{10}CX_6CX_5CXCX_{15}C$	8.11%
$CX_{11}CXCX_5C$	5.22%
$CX_{11}CX_5CX_5CXCX_7C$	2.56%
$CX_{10}CX_6CX_5CXCX_{13}C$	1.47%
$CX_{10}CX_5CXCX_4CX_8C$	1.19%
$CX_{10}CX_6CX_6CXCX_7C$	1.08%
$CX_{10}CX_4CX_7CXCX_8C$	1.05%
$CX_{10}CX_4CX_7CXCX_7C$	0.91%
$CX_{13}CX_8CX_8C$	0.91%
$CX_{10}CX_6CX_5CXCX_7C$	0.59%
$CX_{10}CX_5CX_5C$	0.57%
$CX_{10}CX_5CX_6CXCX_7C$	0.50%
$CX_{10}CX_6CX_5CX_7CX_9C$	0.43%
$CX_9CX_7CX_5CXCX_7C$	0.41%
$CX_{10}CX_6CX_5CXCX_9C$	0.36%
$CX_{10}CXCX_4CX_5CX_{11}C$	0.32%
$CX_7CX_3CX_6CX_5CXCX_5CX_{10}C$	0.32%
$CX_{10}CXCX_4CX_5CXCX_2CX_3C$	0.30%
$CX_{16}CX_5CXC$	0.23%

Cysteine pattern (MID10)	
$CX_{10}CXCX_4CX_5CXCX_2CX_3C$	2.87%
$CX_{10}CX_5CX_5C$	0.73%
$CX_{10}CXCX_4CX_5CX_{11}C$	0.67%
$CX_6CX_4CXCX_4CX_5C$	0.61%
$CX_{11}CX_4CX_5CX_6CX_3C$	0.55%
$CX_8CX_2CX_6CX_5C$	0.43%
$CX_{10}CX_5CX_5CXCX_{10}C$	0.37%
$CX_{10}CXCX_6CX_4CXC$	0.31%
$CX_{10}CX_5CX_5CXCX_2C$	0.31%
$CX_{14}CX_2CX_3CXCXC$	0.31%
$CX_{15}CX_5CXC$	0.31%
$CX_4CX_6CX_9CX_2CX_{11}C$	0.31%
$CX_6CX_4CX_5CX_5CX_{12}C$	0.31%
$CX_7CX_3CXCXCX_4CX_5CX_9C$	0.31%
$CX_{10}CX_6CX_5C$	0.24%
$CX_7CX_3CX_5CX_5CX_9C$	0.24%
$CX_7CX_5CXCX_2C$	0.24%
$CX_{10}CXCX_6C$	0.18%
$CX_{10}CX_3CX_3CX_5CX_7CXCX_6C$	0.18%
$CX_{10}CX_4CX_5CX_{12}CX_2C$	0.18%

Cysteine pattern (MID11)

$CX_{12}CX_4CX_5CXCXCX_9CX_3C$	1.19%
$CX_{12}CX_4CX_5CX_{12}CX_2C$	0.96%
$CX_{10}CX_6CX_5CXCX_{11}C$	0.92%
$CX_{16}CX_5CXCXCX_{14}C$	0.70%
$CX_{10}CX_5CXCX_8CX_6C$	0.52%
$CX_{12}CX_4CX_5CX_8CX_2C$	0.49%
$CX_{12}CX_5CX_5CXCX_8C$	0.47%
$CX_{10}CX_6CX_5CXCX_4CXCX_9C$	0.45%
$CX_{11}CX_4CX_5CX_8CX_2C$	0.45%
$CX_{10}CX_6CX_5CX_8CX_2C$	0.43%
$CX_{10}CX_6CX_5CXCX_8C$	0.36%
$CX_{10}CX_6CX_5C$	0.31%
$CX_{10}CX_6CX_5CXCX_3CX_8CX_2C$	0.29%
$CX_{10}CX_6CX_5CX_3CX_8C$	0.29%
$CX_{10}CX_6CX_5CXCX_2CX_6CX_5C$	0.25%
$CX_7CX_6CX_3CX_3CX_9C$	0.25%
$CX_9CX_8CX_5CX_6CX_5C$	0.22%
$CX_{10}CX_2CX_2CX_7CXCX_{11}CX_5C$	0.20%
$CX_{10}CX_6CX_5CXCX_{13}C$	0.20%
$CX_{10}CX_6CX_5CXCX_2CX_8CX_4C$	0.20%

Representative examples of cysteine patterns are shown for each deep sequencing run. The cysteines in the CDR H3 regions were symbolized as "C". The amino acids between two cysteines were symbolized as "X_n".

Table S6. Diversity Mechanisms in Mouse, Human, and Bovine Antibody Systems, Related to Figure 7

Diversity Mechanism	***Mouse/Human***	***Bovine Ultralong***
Combinatorial	V(D)J recombination V_H-V_L pairing	Limited
Junctional	Length variation in CDR H3 loops	Stalk length and orientation
Somatic Hypermutation	antibody affinity enhancement	Structural diversity in CDR H3 stalk and knob through cysteine variation and alterations in disulfide pattern

Table S7. Oligos for H12 Knob Modification, Related to Figure 6

Oligo #	Oligo Name	5'- Sequence - 3'
701	Fwd KO BsaI(1) H12	ACTGGGATGCCTGGTGTCAAGCTATATGCCCGAGCCT
702	Rev KO BsaI(1) H12	GGGCATATAGCTTGACACCAGGCATCCCAGTGTCACG
703	Fwd KO BsaI(2) H12	AGTACAAGTGCAAGGTGTCCAACAAAGCCCTCCCAGC
704	Rev KO BsaI(2) H12	AGGGCTTTGTTGGACACCTTGCACTTGTACTCCTTGCC
705	Fwd Knob-KO BsaI H12	GAGACCTACTATGGTTCGGGTCTCATCACTACTTATACTTACGAACA
706	Rev Knob-KO BsaI H12	GAGACCCGAACCATAGTAGGTCTCACTGGATTGTTGGGTCGTCT
707	Fwd SGSintoH12	CCAGTAGCGGCTCAA
708	Rev SGSintoH12	GTGATTGAGCCGCTA
709	Fwd SGGSintoH12	CCAGTAGCGGCGGTTCAA
710	Rev SGGSintoH12	GTGATTGAACCGCCGCTA
711	Fwd H12 109-117 BsaI	CCAGTTGTGAGACCTACTATGGTTCGGGTCTCTGTACCCCGGGTCCTG AGAGTTGTTGTCGGAGTGGTTGTGACGGTGCTCGGAGGCGTGTTGGAC TGCGTTATTTTTTTGATTCGACTAGTCCAA
712	Rev H12 109-117 BsaI	GTGATTGGACTAGTCGAATCAAAAAAATAACGCAGTCCAACACGCCTC CGAGCACCGTCACAACCACTCCGACAACAACTCTCAGGACCCGGGGTA CAGAGACCCGAACCATAGTAGGTCTCACAA
713	Fwd H12 119-129 BsaI	CCAGTTGTCCTGCGGGTTTTCGTGATTGTGTTGCTTGTGAGACCTACT ATGGTTCGGGTCTCTGTGACGGTGCTCGGAGGCGTGTTGGACTGCGTT ATTTTTTTGATTCGACTAGTCCAA
714	Rev H12 119-129 BsaI	GTGATTGGACTAGTCGAATCAAAAAAATAACGCAGTCCAACACGCCTC CGAGCACCGTCACAGAGACCCGAACCATAGTAGGTCTCACAAGCAACA CAATCACGAAAACCCGCAGGACAA
715	Rev H12 131-148 BsaI	CCAGTTGTCCTGCGGGTTTTCGTGATTGTGTTGCTTGTACCCCGGGTC CTGAGAGTTGTTGTCGGAGTGGTTGTGAGACCTACTATGGTTCGGGTC TCA
716	Fwd H12 131-148 BsaI	GTGATGAGACCCGAACCATAGTAGGTCTCACAACCACTCCGACAACAA CTCTCAGGACCCGGGGTACAAGCAACACAATCACGAAAACCCGCAGGA CAA

Point Mutation	Fwd oligo 5'-Sequence-3'
P109A	GTTGTGCCGCGGGTTTTCGTGATTGTGTTGCTT
A110Y	GTTGTCCTTACGGTTTTCGTGATTGTGTTGCTT
G111A	GTTGTCCTGCGGCCTTTCGTGATTGTGTTGCTT
F112A	GTTGTCCTGCGGGTGCCCGTGATTGTGTTGCTT
R113A	GTTGTCCTGCGGGTTTTGCCGATTGTGTTGCTT
D114A	GTTGTCCTGCGGGTTTTCGTGCCTGTGTTGCTT
C115A	GTTGTCCTGCGGGTTTTCGTGATGCCGTTGCTT
V116A	GTTGTCCTGCGGGTTTTCGTGATTGTGCCGCTT
A117Y	GTTGTCCTGCGGGTTTTCGTGATTGTGTTGCCT
T119A	CTTGTGCCCCGGGTCCTGAGAGTTGTTGTCGGAGTGGTT
P120A	CTTGTACCGCCGGTCCTGAGAGTTGTTGTCGGAGTGGTT
G121A	CTTGTACCCCGGCCCCTGAGAGTTGTTGTCGGAGTGGTT

P122A	CTTGTACCCCGGGTGCCGAGAGTTGTTGTCGGAGTGGTT
E123A	CTTGTACCCCGGGTCCTGCCAGTTGTTGTCGGAGTGGTT
S124A	CTTGTACCCCGGGTCCTGAGGCCTGTTGTCGGAGTGGTT
C125A	CTTGTACCCCGGGTCCTGAGAGTGCCTGTCGGAGTGGTT
C126A	CTTGTACCCCGGGTCCTGAGAGTTGTGCCCGGAGTGGTT
R127A	CTTGTACCCCGGGTCCTGAGAGTTGTTGTGCCAGTGGTT
S128A	CTTGTACCCCGGGTCCTGAGAGTTGTTGTCGGGCCGGTT
G129A	CTTGTACCCCGGGTCCTGAGAGTTGTTGTCGGAGTGCCT
D131A	GTTGTGCCGGTGCTCGGAGGCGTGTTGGACTGCGTTATTTTTTTGATTCGACTAGTCCAA
G132A	GTTGTGACGCCGCTCGGAGGCGTGTTGGACTGCGTTATTTTTTTGATTCGACTAGTCCAA
A133Y	GTTGTGACGGTTACCGGAGGCGTGTTGGACTGCGTTATTTTTTTGATTCGACTAGTCCAA
R134A	GTTGTGACGGTGCTGCCAGGCGTGTTGGACTGCGTTATTTTTTTGATTCGACTAGTCCAA
R135A	GTTGTGACGGTGCTCGGGCCCGTGTTGGACTGCGTTATTTTTTTGATTCGACTAGTCCAA
R136A	GTTGTGACGGTGCTCGGAGGGCCGTTGGACTGCGTTATTTTTTTGATTCGACTAGTCCAA
V137A	GTTGTGACGGTGCTCGGAGGCGTGCCGGACTGCGTTATTTTTTTGATTCGACTAGTCCAA
G138A	GTTGTGACGGTGCTCGGAGGCGTGTTGCCCTGCGTTATTTTTTTGATTCGACTAGTCCAA
L139A	GTTGTGACGGTGCTCGGAGGCGTGTTGGAGCCCGTTATTTTTTTGATTCGACTAGTCCAA
R140A	GTTGTGACGGTGCTCGGAGGCGTGTTGGACTGGCCTATTTTTTTGATTCGACTAGTCCAA
Y141A	GTTGTGACGGTGCTCGGAGGCGTGTTGGACTGCGTGCCTTTTTTGATTCGACTAGTCCAA
F142A	GTTGTGACGGTGCTCGGAGGCGTGTTGGACTGCGTTATGCCTTTGATTCGACTAGTCCAA
F143A	GTTGTGACGGTGCTCGGAGGCGTGTTGGACTGCGTTATTTTGCCGATTCGACTAGTCCAA
D144A	GTTGTGACGGTGCTCGGAGGCGTGTTGGACTGCGTTATTTTTTTGCCTCGACTAGTCCAA
S145A	GTTGTGACGGTGCTCGGAGGCGTGTTGGACTGCGTTATTTTTTTGATGCCACTAGTCCAA
T146A	GTTGTGACGGTGCTCGGAGGCGTGTTGGACTGCGTTATTTTTTTGATTCGGCCAGTCCAA
S147A	GTTGTGACGGTGCTCGGAGGCGTGTTGGACTGCGTTATTTTTTTGATTCGACTGCCCCAA
P148A	GTTGTGACGGTGCTCGGAGGCGTGTTGGACTGCGTTATTTTTTTGATTCGACTAGTGCCA
Point Mutation	Reverse oligo 5'-Sequence-3'
P109A	GTACAAGCAACACAATCACGAAAACCCGCGGCA
A110Y	GTACAAGCAACACAATCACGAAAACCGTAAGGA
G111A	GTACAAGCAACACAATCACGAAAGGCCGCAGGA
F112A	GTACAAGCAACACAATCACGGGCACCCGCAGGA
R113A	GTACAAGCAACACAATCGGCAAAACCCGCAGGA
D114A	GTACAAGCAACACAGGCACGAAAACCCGCAGGA
C115A	GTACAAGCAACGGCATCACGAAAACCCGCAGGA
V116A	GTACAAGCGGCACAATCACGAAAACCCGCAGGA
A117Y	GTACAGGCAACACAATCACGAAAACCCGCAGGA
T119A	TCACAACCACTCCGACAACAACTCTCAGGACCCGGGGCA
P120A	TCACAACCACTCCGACAACAACTCTCAGGACCGGCGGTA
G121A	TCACAACCACTCCGACAACAACTCTCAGGGGCCGGGGTA
P122A	TCACAACCACTCCGACAACAACTCTCGGCACCCGGGGTA
E123A	TCACAACCACTCCGACAACAACTGGCAGGACCCGGGGTA
S124A	TCACAACCACTCCGACAACAGGCCTCAGGACCCGGGGTA
C125A	TCACAACCACTCCGACAGGCACTCTCAGGACCCGGGGTA
C126A	TCACAACCACTCCGGGCACAACTCTCAGGACCCGGGGTA
R127A	TCACAACCACTGGCACAACAACTCTCAGGACCCGGGGTA
S128A	TCACAACCGGCCCGACAACAACTCTCAGGACCCGGGGTA
G129A	TCACAGGCACTCCGACAACAACTCTCAGGACCCGGGGTA
D131A	GTGATTGGACTAGTCGAATCAAAAAAATAACGCAGTCCAACACGCCTCCGAGCACCGGCA
G132A	GTGATTGGACTAGTCGAATCAAAAAAATAACGCAGTCCAACACGCCTCCGAGCGGCGTCA

A133Y	GTGATTGGACTAGTCGAATCAAAAAAATAACGCAGTCCAACACGCCTCCGGTAACCGTCA
R134A	GTGATTGGACTAGTCGAATCAAAAAAATAACGCAGTCCAACACGCCTGGCAGCACCGTCA
R135A	GTGATTGGACTAGTCGAATCAAAAAAATAACGCAGTCCAACACGGGCCCGAGCACCGTCA
R136A	GTGATTGGACTAGTCGAATCAAAAAAATAACGCAGTCCAACGGCCCTCCGAGCACCGTCA
V137A	GTGATTGGACTAGTCGAATCAAAAAAATAACGCAGTCCGGCACGCCTCCGAGCACCGTCA
G138A	GTGATTGGACTAGTCGAATCAAAAAAATAACGCAGGGCAACACGCCTCCGAGCACCGTCA
L139A	GTGATTGGACTAGTCGAATCAAAAAAATAACGGGCTCCAACACGCCTCCGAGCACCGTCA
R140A	GTGATTGGACTAGTCGAATCAAAAAAATAGGCCAGTCCAACACGCCTCCGAGCACCGTCA
Y141A	GTGATTGGACTAGTCGAATCAAAAAAGGCACGCAGTCCAACACGCCTCCGAGCACCGTCA
F142A	GTGATTGGACTAGTCGAATCAAAGGCATAACGCAGTCCAACACGCCTCCGAGCACCGTCA
F143A	GTGATTGGACTAGTCGAATCGGCAAAATAACGCAGTCCAACACGCCTCCGAGCACCGTCA
D144A	GTGATTGGACTAGTCGAGGCAAAAAAATAACGCAGTCCAACACGCCTCCGAGCACCGTCA
S145A	GTGATTGGACTAGTGGCATCAAAAAAATAACGCAGTCCAACACGCCTCCGAGCACCGTCA
T146A	GTGATTGGACTGGCCGAATCAAAAAAATAACGCAGTCCAACACGCCTCCGAGCACCGTCA
S147A	GTGATTGGGGCAGTCGAATCAAAAAAATAACGCAGTCCAACACGCCTCCGAGCACCGTCA
P148A	GTGATGGCACTAGTCGAATCAAAAAAATAACGCAGTCCAACACGCCTCCGAGCACCGTCA